Geobiology

Geobiology (2014), **12**, 231–249 DOI: 10.1111/gbi.12079

Functional gene diversity of oolitic sands from Great Bahama Bank

M. R. DIAZ,[1] J. D. VAN NORSTRAND,[2] G. P. EBERLI,[3] A. M. PIGGOT,[3] J. ZHOU[2] AND J. S. KLAUS[1,4]

[1]*Marine Biology and Fisheries, Rosenstiel School of Marine and Atmospheric Science, University of Miami, Miami, FL, USA*
[2]*Department of Microbiology and Plant Biology, Institute for Environmental Genomics, University of Oklahoma, Norman, OK, USA*
[3]*Marine Geology and Geophysics, Rosenstiel School of Marine and Atmospheric Science, University of Miami, Miami, FL, USA*
[4]*Department of Geological Sciences, University of Miami, Coral Gables, FL, USA*

ABSTRACT

Despite the importance of oolitic depositional systems as indicators of climate and reservoirs of inorganic C, little is known about the microbial functional diversity, structure, composition, and potential metabolic processes leading to precipitation of carbonates. To fill this gap, we assess the metabolic gene carriage and extracellular polymeric substance (EPS) development in microbial communities associated with oolitic carbonate sediments from the Bahamas Archipelago. Oolitic sediments ranging from high-energy 'active' to lower energy 'non-active' and 'microbially stabilized' environments were examined as they represent contrasting depositional settings, mostly influenced by tidal flows and wave-generated currents. Functional gene analysis, which employed a microarray-based gene technology, detected a total of 12 432 of 95 847 distinct gene probes, including a large number of metabolic processes previously linked to mineral precipitation. Among these, gene-encoding enzymes for denitrification, sulfate reduction, ammonification, and oxygenic/anoxygenic photosynthesis were abundant. In addition, a broad diversity of genes was related to organic carbon degradation, and N_2 fixation implying these communities has metabolic plasticity that enables survival under oligotrophic conditions. Differences in functional genes were detected among the environments, with higher diversity associated with non-active and microbially stabilized environments in comparison with the active environment. EPS showed a gradient increase from active to microbially stabilized communities, and when combined with functional gene analysis, which revealed genes encoding EPS-degrading enzymes (chitinases, glucoamylase, amylases), supports a putative role of EPS-mediated microbial calcium carbonate precipitation. We propose that carbonate precipitation in marine oolitic biofilms is spatially and temporally controlled by a complex consortium of microbes with diverse physiologies, including photosynthesizers, heterotrophs, denitrifiers, sulfate reducers, and ammonifiers.

Received 30 August 2013; accepted 22 January 2014

Corresponding author: M. R. Diaz. Tel.: +1 305-421-4879; fax: +1 305-421-4600; e-mail: mdiaz@rsmas.miami.edu

INTRODUCTION

Oolitic sands are one of the predominant sediment types comprising tropical carbonate platforms of both the modern and geologic past. While oolitic sand grains vary in both structure and mineralogy, the majority of modern marine ooids range in size from 0.25 to 2 mm and are formed by concentric layers of tangentially arranged aragonite needles around a nucleus. Oolitic sands are generally formed in agitated shallow waters favored by either intertidal or subtidal conditions, which creates bidirectional currents emulating a 'spin cycle' where oolitic sands are temporarily trapped (Rankey *et al.*, 2006). Modern marine ooids are found in the Bahamas (Ball, 1967; Harris, 1979), the Yucatán (Ward & Brady, 1973), the Arabian Gulf (Loreau & Purser, 1973), the South Pacific (Rankey & Reeder, 2009) and Shark Bay, Australia (Davies, 1970). In the Bahamas, hundreds of square meters of oolitic sands form extensive bank and shoal-water complexes with carbonate accumulation estimated at 3.2 GT per year (Milliman, 1993; Milliman &

Droxler, 1995; Harris, 2010). These oolitic sand bodies are characterized by high porosity and permeability, enabling advective exchange of particles and dissolved materials in the overlying water column.

Despite the extent and importance of oolitic grainstones in many ancient carbonate successions (Keith & Zuppann, 1993) including large hydrocarbon reservoirs (Benson, 1988; Lindsay *et al.*, 2006), the genesis of ooids remains controversial. While various theories support abiotic processes (Morse & Mackenzie, 1990; Duguid *et al.*, 2010), others attribute ooid genesis to biogenic factors (Davies *et al.*, 1978; Gerdes *et al.*, 1994; Plée *et al.*, 2008, 2010; Pacton *et al.*, 2012), some of which are supported by the presence of nanoscale textures of bacterial origin (Folk & Lynch, 2001), and conspicuous presence of organic material (e.g., aspartic acid, lipids) incorporated during ooid cortex growth (Mitterer, 1968; Summons *et al.*, 2013). Despite evidence of biologic origin, the role of microbes in the accretion of ooids has been challenged due to endolithic micro-organisms with capabilities for micritization in ooid cortices and cement precipitation in the borings (Duguid *et al.*, 2010). Notwithstanding, what is still debatable is whether precipitation processes in the cortical layers of the ooids are locally induced by microbial activities. There is growing evidence that microbes can control the degree of carbonate saturation on their surroundings through their metabolic activities, some of which lead to the formation of alkaline microenvironments (Kahle, 2007; Plée *et al.*, 2008, 2010). The formation of these alkaline microenvironments can thus induce carbonate precipitation. The extent of carbonate precipitation is thus the result of the net balance of microbial processes that promote precipitation (e.g., photosynthesis, anoxygenic photoautotrophy, sulfate reduction, denitrification, ammonification) and those that promote dissolution of carbonate (e.g., aerobic respiration, sulfide oxidation, fermentation) (Castanier *et al.*, 2000; Visscher & Stolz, 2005; Ries *et al.*, 2008). Previous studies on microbial systems in the Bahamas suggest carbonate precipitation in chalky aragonite muds west of Andros Island, Bahamas (whitings), to be mostly driven by the action of denitrifiers on the calcium salts present in seawater (Drew, 1911, 1914), whereas others propose photosynthesizers (e.g., *Synechococcus*) as the main drivers (Robbins *et al.*, 1996). The synergism between sulfate reducers, heterotrophs, and phototrophs (e.g., cyanobacteria) has also been implicated as drivers of carbonate precipitation in stromatolites and microbial mat systems in the Bahamas (Dupraz *et al.*, 2004; Dupraz & Visscher, 2005) and, most recently, in ooid formation (Diaz *et al.*, 2013; Summons *et al.*, 2013).

Extracellular polymeric substances (EPS) have also been shown to contribute to carbonate precipitation (Visscher *et al.*, 1999; Dupraz & Visscher, 2005; Dupraz *et al.*, 2009); as such, different types of EPS alteration are known to induce calcification, for example, microbially mediated decomposition by heterotrophs, organomineralization, and UV decomposition (Dupraz & Visscher, 2005). The EPS matrix, which is produced by a consortia of heterotrophs, sulfate reducers, and cyanobacteria, can sequester nutrients from the environment and provide protection from fluctuations in temperature, desiccation, UV radiation, and predation (Decho, 1990, 2000; Davey & O'Toole, 2000). In addition, EPS can assist in the development of microenvironments, where sharp geochemical gradients occur by the binding of organic molecules and ions to the cell matrix. While EPS can inhibit precipitation when trapping free divalent cations (Mg^{+2}, Ca^{+2}) in the organic matrix (Kawaguchi & Decho, 2002; Braissant *et al.*, 2009), microbial degradation of EPS releases bound Ca^{+2}, favoring the development of 'hot spots' where localized $CaCO_3$ occur (Dupraz & Visscher, 2005; Baumgartner *et al.*, 2006). The role of EPS and associated microbes in the accretion, lamination, and lithification of modern stromatolites has been well documented and represents a good model of the importance of microbes in calcification processes (Dupraz & Visscher, 2005; Baumgartner *et al.*, 2006).

Apart from recent molecular phylogenetic studies that shows marine oolitic grains harbor a remarkably diverse bacterial community, represented by *Proteobacteria* within the *Alpha-*, *Delta-* and *Gamma*-lineages, *Cyanobacteri*a, *Planctomycetes*, and several other groups (Diaz *et al.*, 2013; Edgcomb *et al.*, 2013), little is known about the functional gene diversity and metabolic potential of these communities. To circumvent this, we employ a functional gene microarray, GEOCHIP 4.2 as well as EPS analysis on oolitic grains from high-energy 'active' environments (tidal currents) to lower energy 'non-active' and 'microbially stabilized' environments of the Bahamas. GEOCHIP 4.2 is a high-density oligonucleotide-based microarray that contains 95 847 distinct probes covering 246 285 coding sequences for 740 gene categories associated with microbial functional processes including carbon, nitrogen, sulfur, and phosphorus cycling, energy processing, metal resistance and reduction, organic contaminant degradation, stress responses, antibiotic resistance, and bacterial phages (Table S1). The GEOCHIP 4.2 microbial domain includes 4322 species of bacteria, 188 species of archaea, 420 eukaryotes (fungi), and 273 bacteriophages. In view of the high-throughput qualitative and quantitative capabilities of the method (Wang *et al.*, 2011a), this functional gene array technology is becoming an important tool for studying biogeochemical processes and putative functions of microbial communities (Bai *et al.*, 2012; Chan *et al.*, 2013; Zhang *et al.*, 2013). The goal of this study is to characterize the functional gene diversity and metabolic potential of microbial communities in oolitic sands of the Bahamas from three different contrasting environments, and how their functional capabilities relate to biogeochemical processes, including carbonate precipitation.

MATERIALS AND METHODS

Sample sites and sample collection

The Bahamas Archipelago comprises 470 000 km^2 and is located between 20 ° and 28 °N at the southeastern continental margin of the North America Plate. The area is characterized by isolated carbonate platforms (over an area of 5 km) with over 600 cays and shoal-water complexes of ooids that form margin parallel marine sand belts, tidal bar belts, or platform interior blankets (Ball, 1967). Sea surface temperatures range from 23 to 26 °C in the northern archipelago, whereas in the southern end, the temperatures range from 25 to 29 °C (Gaudain & Medley, 2000; Antonov *et al*., 2006). Salinity in this area fluctuates from 36 ppm to 37 ppm. The hydrodynamics of the platforms result from the interaction of waves, wind, and tides (Reeder & Rankey, 2008). The shallow water (9 < 10 m) ooid shoal complexes in Great Bahama Bank are shaped daily by tidal currents with velocities that can exceed 100 cm s^{-1} (Rankey *et al*., 2006; Reeder & Rankey, 2008). Due to the relatively shallow water depths on the platforms, the water volume exchange during diurnal and semidiurnal tidal cycles is often magnified as water flows through narrow channels. Sampling locations are illustrated in Fig. 1 and include three different types of ooid shoals comprising ooids with mean grain size ranging from 350 to 500 μm: Cat Cay, represented by a bank margin sand belt; Joulters Cay, a tidal bar belt; and Shroud Cay, a tidal delta. These extensively studied areas were selected as they display a variety of depositional environments in which ooid sands can accumulate and because their facies share similarities with ancient carbonate sand bodies (Cruz, 2008; Harris, 2010; Petrie, 2010).

Independent of the shoal morphology, which can resemble tidal bar belts and marine sand belts, ooid shoal complexes typically have three environments, herein described as: (i) active ooid shoal; (ii) non-active ooid; and (iii) microbially stabilized ooids (Fig. 2). In the active portion of the complex, tidal currents or wave action constantly move the ooids. The crests of these active ooid shoals are characterized by high hydrodynamic energy with well-sorted oolitic grains consisting of up to 90% ooids. Adjacent to the shoal is transition zones that experience a less intense hydrodynamic regime, herein described as non-active ooid areas. These areas flank the shoal crests and lie in deeper waters (~1–3 m). The grains are poorly sorted and composed of ooid sands (60–80%) with some admixtures of peloids (20–40%) and skeletal grains (5%). Some of these areas could be associated with a sparse and/or discontinuous covering of individual sea grass plants (e.g., *Thalassia*). Other zones, herein described as microbially stabilized, are located in low areas on the crest of the shoals or tidal flats and are characterized by the presence of microbial biofilm or fine filamentous cyanobacterial coatings providing some level of ooid stabilization. Hydrodynamic flow rates in these more physically stable areas can be as slow as 2 cm s^{-1} (Smith, 1995).

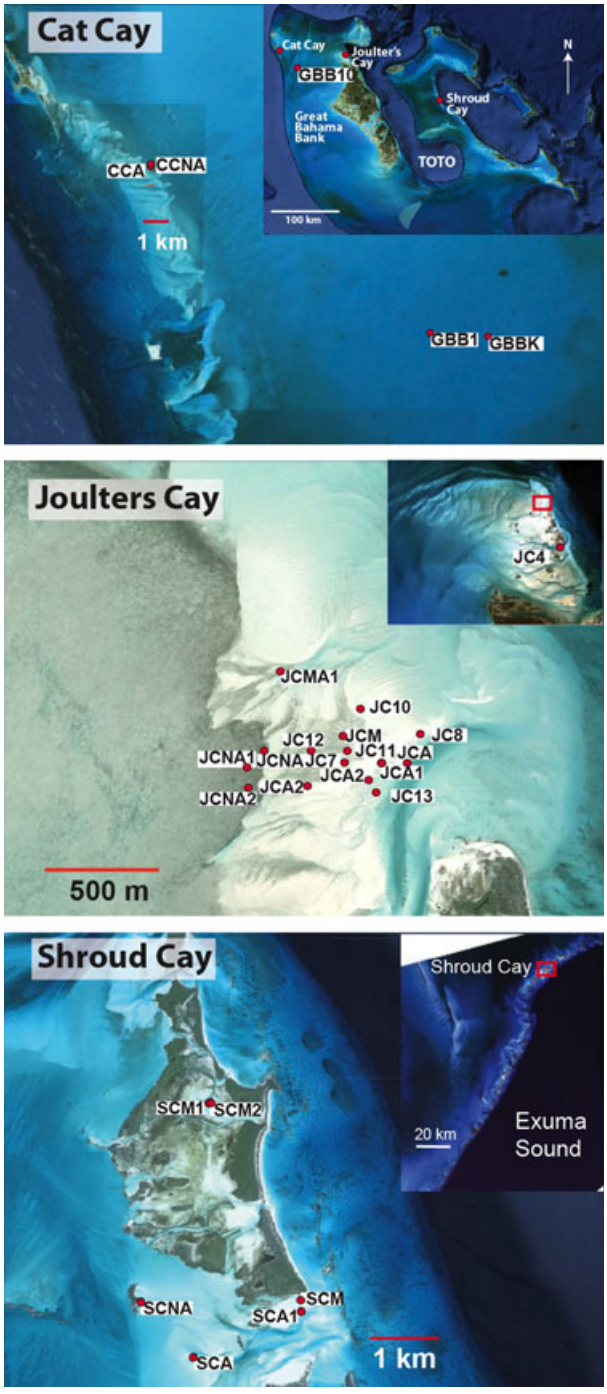

Fig. 1 Detailed map of sampling localities in the Great Bahamas. Red box outlines the sample areas.

Samples were collected during various expeditions aboard the R/V Coral Reef in June–July of 2010 and June 2012 in three main areas (Table 1). The Cat Cay ooid shoal forms a narrow (1–3 km wide) margin parallel marine sand belt of

Fig. 2 Representative photographs of the Joulter's Cay oolitic shoal complex (A–G) and of the microbially stabilized area of Shroud Cay (H). (A) Overview of active area in JoultersCay; (B) Underwater close-up of ooids in motion; (C) Non-active area of Joulters Cay with the active area (white) in background; (D) *Thalassia* sea grass colonizing the non-active area; (E) Microbially stabilized environment of Joulters Cay with fine filamentous, microbial coating; (F) close-up of microbially stabilized ooids; (G) gradual increase in microbially stabilization on Joulters Cay from fine filamentous coating (foreground) to mat-like coating (dark background); (H) microbially stabilized area at Shroud Cay.

approximately 15 km length on the western margin of Great Bahama Bank (Cruz, 2008). Maximum tidal range is 119 cm, and tidal flow velocities vary during flood tide (<80 cm s^{-1}) and ebb tide (<40 cm s^{-1}). The surface sediments of the Cat Cay ooid shoal are composed of moderately well-sorted, medium sand ooid/peloidal grains with a mean grain size of 361 ± 44 μm. Samples for this study were collected from a flood tidal delta lobe that has not migrated for over 60 years and where ooids are assumed to be forming today. The sediments are composed of ooids (47%) and peloids (53%), and scattered skeletal grains (Cruz, 2008). A second sample was taken about 50 m from the lobe toward the platform interior in an environment with fine to very fine and muddy peloidal sand stabilized by seagrass (Cruz, 2008).

The Joulters Cay shoal complex is located north of the Andros Island. The 400 km^2 sand flat is cut by tidal channels and fringed by mobile sand belts (Harris, 1979, 1983) consisting of well-sorted ooids (mean grain size of 350–500 μm) moved by tidal currents with velocities that exceed 100 cm s^{-1}. Samples were collected from the northeastern part of the Joulters Cay shoal on a large (several square kilometers) frontal sand bar with active ooid formation in the intertidal zone. Here, the sediments are over 90% ooids (Fig. 3A, B). Fine filamentous cyanobacteria and/or mucilaginous microbial coatings stabilize some areas on this lobe where samples were collected (Figs 2E,F and 3E,F). Toward the upper intertidal zone, the filamentous coating becomes thicker and develops a more coherent structure (Fig. 2G). To the west of the active sand bar is a large sand flat area that

Table 1 Characterization and locality information of sediment samples analyzed for functional gene and extracellular polymeric substance (EPS) analysis

Sample	Region	Environment	Sediment type	Latitude	Longitude
GBB10	Great Bahama Bank	Non-active	Ooid pelletoidal grainstone	25.29165	−78.84259
GBBK	Great Bahama Bank	Non-active	Ooid pelletoidal packstone	25.42896	−79.03449
JC4	Joulters Cay, Great Bahama Bank	Active	Ooid grainstone	25.27343	−78.12161
JC7	Joulters Cay, Great Bahama Bank	Microbially stabilized	Ooid pelletoidal	25.33497	−78.14612
JC8	Joulters Cay, Great Bahama Bank	Active	Ooid grainstone	25.33628	−78.14311
JC10	Joulters Cay, Great Bahama Bank	Active	Ooid grainstone	25.33610	−78.14508
JC11	Joulters Cay, Great Bahama Bank	Microbially stabilized	Ooid grainstone	25.33566	−78.14607
JC12	Joulters Cay, Great Bahama Bank	Microbially stabilized	Ooid grainstone	25.33513	−78.14778
JC13	Joulters Cay, Great Bahama Bank	Non-active	Ooid grainstone	25.33446	−78.15049
JCA	Joulters Cay, Great Bahama Bank	Active	Ooid pelletoidal grainstone	25.335222	−78.143583
JCA1	Joulters Cay, Great Bahama Bank	Active	Ooid grainstone	25.335778	−78.144667
JCA2	Joulters Cay, Great Bahama Bank	Active	Ooid grainstone	25.334562	−78.145247
JCNA	Joulters Cay, Great Bahama Bank	Non-active	Ooid grainstone packstone	25.335722	−78.149806
JCNA1	Joulters Cay, Great Bahama Bank	Non-active	Ooid grainstone packstone	25.335111	−78.150556
JCNA2	Joulters Cay, Great Bahama Bank	Non-active	Ooid grainstone packstone	25.334278	−78.1505
JCM	Joulters Cay, Great Bahama Bank	Microbially stabilized	Ooid grainstone packstone	25.336306	−78.146361
JCMA1	Joulters Cay, Great Bahama Bank	Microbially stabilized	Ooid grainstone packstone	25.338894	−78.149106
JCMA2	Joulters Cay, Great Bahama Bank	Microbially stabilized	Ooid grainstone packstone	25.333864	−78.147915
SCA	Shroud Cay, Great Bahama Bank	Active	Ooid grainstone	24.507194	−76.783778
SCA1	Shroud Cay, Great Bahama Bank	Active	Ooid grainstone	24.513528	−76.767444
SCNA	Shroud Cay, Great Bahama Bank	Non-active	Ooid grainstone	24.514861	−76.791917
SCM	Shroud Cay, Great Bahama Bank	Microbially stabilized	Ooid grainstone packstone	24.515111	−76.767472
SCM1	Shroud Cay, Great Bahama Bank	Microbially stabilized	Ooid grainstone packstone	24.542639	−76.781361
SCM2	Shroud Cay, Great Bahama Bank	Microbially stabilized	Ooid grainstone packstone	24.542617	−76.781533
GBB1	Great Bahama Bank	Non-active	Ooid grainstone packstone	25.429306	−79.064417
CCA	Cat Cay, Great Bahama Bank	Active	Ooid grainstone	25.508066	−79.210466
CCNA	Cat Cay, Great Bahama Bank	Non-active	Ooid grainstone packstone	25.509028	−79.210333

Bold font denotes samples analyzed with GEOCHIP 4.2, whereas italic font represents samples used for EPS determinations.

is only exposed at spring low tide and does not appear to have any sand transport, except during storms (Fig. 2C,D). In this inactive part of the shoal, the sedimentary facies are often associated with sea grasses and consist of ooids (30–70%) with a mixture of skeletal (5–20%), peloidal sand (20–40%), and carbonate mud (up to 20%) (Fig. 3C,D). Most of the peloids are micritized ooids.

The third study area is at Shroud Cay in the Exumas along the 180-km-long margin a series of ooid tidal deltas exist between islands (Harris, 2010). These deltas form as lateral flow is restricted because of the presence of islands, and tidal currents are concentrated through the channels with maximal tidal velocities of 200 cm s^{-1} (González & Eberli, 1997; Rankey *et al.*, 2006; Reeder & Rankey, 2008; Harris, 2010). Samples were collected from the active portions of the flood and ebb tidal deltas south of Shroud Cay. The medium to well-sorted sand consists of ooids (70% and 84%), peloids (23% and 12%), and few skeletal and composite grains (2% and 4%) (Petrie, 2010). Samples were taken from the microbially stabilized areas of the tidal flat adjacent to the active delta (Fig. 2H), where the medium sand-sized sediment is poorly sorted and consists of peloids (51%), ooids (34%), composite grains (13%), and scattered skeletal debris (Petrie, 2010). On the non-active portion of the delta, the composition varies between ooid and peloid dominated sediments with a significant percentage of composite grains (30%) but very little mud (1.3%).

Samples were collected during various expeditions aboard the R/V Coral Reef in June–July of 2010 and June 2012 (Table 1). Approximately 5 g of oolitic sand from the uppermost sediment layer (top 2.5 cm) was collected and transferred into a sterile 50 mL polypropylene tube. While EPS extractions were performed immediately, all other samples were stored at −20 °C until further processing in the laboratory.

DNA isolation and purification

Total community DNA was extracted from 500 mg (wet weight) of sediment using the FastDNA-spin Kit for soil (Q-BIOgene, Carlsbad, CA, USA) and following the manufacturer's protocol. DNA quality was evaluated with a NanoDrop ND-1000 spectrophotometer (NanoDop Technologies Inc, Wilmington, DE, USA). Samples displaying A_{260}:A_{280} ratio >1.7 and A_{260}:A_{230} ratio >1.8 were employed for analysis.

Microbial community genome amplification and labeling

For enhanced sensitivity and genome coverage, purified genomic DNA (25 ng) was amplified in triplicate using

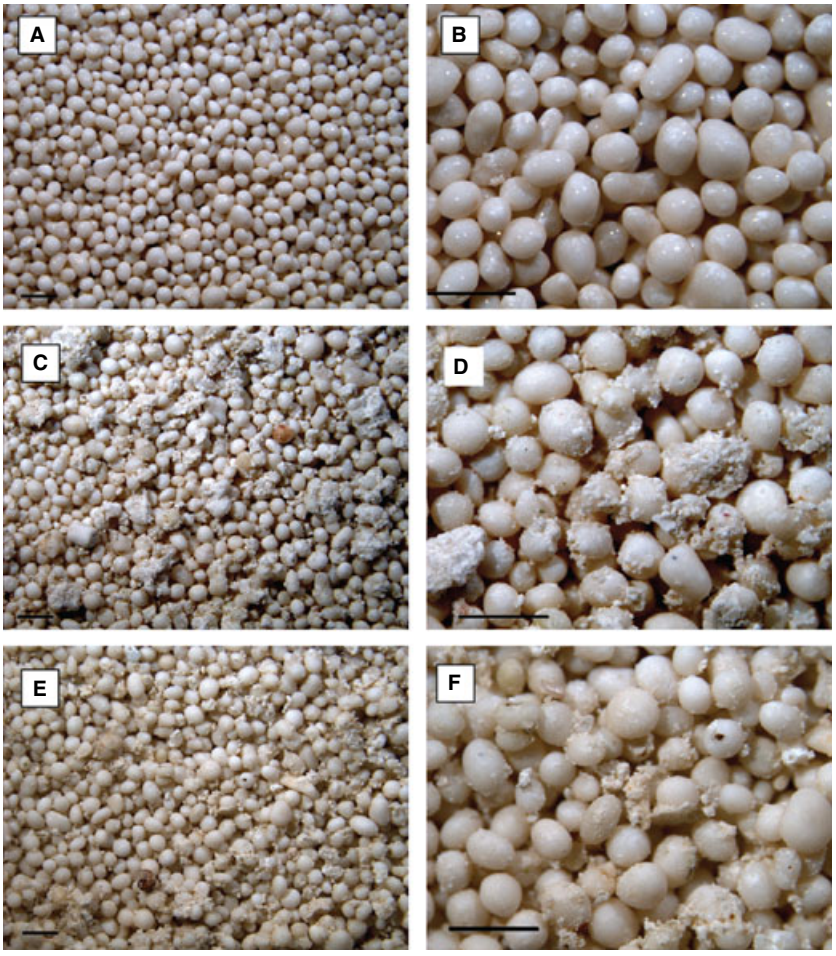

Fig. 3 Oolitic sediments from the Joulter's Cay oolitic shoal complex. (A, B) Highly polished ooids from the active shoal environment (JC4). (C, D) Oolitic sediments from the non-active environment (JC13), including skeletal grains and fine carbonate material. (E, F). Oolitic sediments from the microbially stabilized environment (JC11), including some fine carbonate material. All scale bars = 1 mm.

REPLI-g-Midi kit according to the manufacturer's protocol. This non-PCR-based whole-genome amplification (WGA) uses multiple displacement amplification with random hexamer primers that allows for less-biased DNA amplifications (Wang *et al.*, 2011a). Amplicons were purified with Qiagen QIAquick PCR purification kit (Qiagen, Valencia, CA, USA) following the manufacturer's protocol. The purified amplicon (2 μg) was labeled with a fluorescent dye (Cy5) using random priming with the Klenow fragment of DNA polymerase (Wu *et al.*, 2006). The cocktail labeling mix comprised 1 × random octamer mix (Invitrogen, Carlsbad, CA, USA), 1 mM Cy5 dUTP (Amersham Pharmacia Biotech, Piscataway, NJ, USA), 50 μM (dATP, dCTP, dGTP), 20 μM dTTP (USB Corp., Cleveland, OH, USA), and 40 U of Klenow fragment (Invitrogen). The reactions were incubated at 37 °C for 3 h. The labeled products were further purified with QIAquick PCR purification kit (Qiagen) and dried in a SpeedVAc (45 °C, 45 min).

Hybridization reaction

Two micrograms of dried labeled DNA was suspended in a hybridization solution as described previously (Lu *et al.*, 2012). Duplicate samples were rehydrated with sample tracking control (NimbleGen, Madison, WI, USA) and hybridized in a buffer solution consisting of 40% formamide, 25% SSC, 1% SDS, 2% Cy5-labeled common oligo reference standard (CORS) target, and 2.38% Cy3-labeled alignment oligo (NimbleGen) and 2.8% Cy5-labeled CORS target (Liang *et al.*, 2009). The sample tracking control and CORS are used for identity confirmation and signal normalization/comparison (Liang *et al.*, 2010). The array also incorporates a set of genomic standards to quantitatively analyze gene abundance. DNA samples were denatured at 95 °C for 5 min and hybridized for 16 h at 42 °C on a Maui hybridization station (BioMicro, Salt Lake City, UT, USA). After hybridization, the microarray was scanned at a laser power of 100% (MS200 Microarray Scanner, NimbleGen).

GeoChip data processing and statistical analysis

Pre-processed data were submitted to the Microarray Data Manager (http://ieg.ou.edu/microarray/) to designate the identity of each spot and to determine spot quality. Poor and low quality spots as well as outliers were removed

following Grubbs' test of outliers (Grubbs, 1969). The signal intensities of each spot were normalized across samples by the mean of Cy-5 labeled universal standard signal intensities and then by the mean of Cy-3 labeled signal intensities of all hybridized spots within each sample. Spots with signal-to-noise ratios (SNR) < 2 and replicate outliers (>2 SD) were removed. The signal-to-noise ratio was calculated as: signal intensity − background^{-1} SD. Triplicate samples representing each environment were analyzed.

A natural logarithmic transformation was performed on the two step normalized data (He *et al.*, 2007), prior to submission to GEOCHIP statistical analysis pipeline. Statistical analysis included as follows: microbial diversity indices (e.g., Shannon–Weaver index, Simpson index), detrended correspondence analysis (DCA) for gradient analysis, and three nonparametric tests for multivariate data (e.g., multivariate analysis of variance [Adonis], analysis of similarity [ANOSIM], multiple-response permutation procedure [MRPP]) to assess functional metabolic differences among the environments. Bray and Curtis similarity index was used to calculate the distance matrices for ANOSIM, Adonis, and MRPP. The significant differences were listed as *P*-values. Adonis analyses used the *F*-test based on sequential sums of squares from permutations of the data. *T*-test analysis was conducted to test whether there are significant differences in biofilm abundance.

Extracellular polymeric substance quantification

Extracellular polymeric substance was extracted using a modified protocol of Decho *et al.* (2005). Approximately 2 g of fresh sediment was collected in duplicate at active, non-active, and microbially stabilized sites of Joulters Cay. Each sample was incubated with 0.5 mM EDTA for 15 min at 40 °C, with gentle shaking every 5 min for three consecutive treatments. After each treatment, samples were centrifuged at 8000 × g and the supernatant was pooled. The supernatant was mixed with cold (4 °C) ethanol (final concentration of 70%) for 8 h to precipitate extracted EPS. Quantification of the EPS used the phenol–sulfuric acid method (Underwood *et al.*, 1995; Perkins *et al.*, 2004; Piggot *et al.*, 2012). Absorbance was measured at 490 nm using a spectrophotometer (BioPhotometer plus; Eppendorf, Hamburg, Germany). The amount of polysaccharide present was determined by comparison with a calibration curve using D-glucose. From herein, EPS refers to the bulk polysaccharide fraction of extractable sediment. The sediments were washed with deionized water to remove salts and were dried for the determination of dry weight to calculate the measure of EPS (μg of glucose equivalents g^{-1} dw sed.)

RESULTS

To understand the diversity and functional capabilities of microbial communities associated with ooids, we used a high-throughput functional gene microarray that recovered a total of 12 432 genes, representing ~13% of the total number of genes in the array. Phylogenetically, up to 39 different lineages were documented representing 62 species from archaea, 823 from bacteria, 70 from fungi, and 10 from others (plasmids and uncultured/unidentified prokaryotes). The total number of genes varied significantly between the environments. Active communities retrieved the least number (8631), followed by microbially stabilized (9455) and non-active communities (10 102). Both the Shannon–Weaver (H) and Simpson index (D) indicate higher levels of functional diversity in non-active (H = 9.22; D = 10050), followed by microbially stabilized (H = 9.15; D = 9410.6), and active environments (H = 9.06; D = 8598).

To determine whether different depositional environments harbor distinct patterns of functional gene diversity, DCA was undertaken with all detected functional genes and a group of genes associated with various metabolic processes, for example, denitrification, ammonification, sulfate reduction, carbon degradation, autotrophic CO_2 fixation, methanogenesis, and acetogenesis (Fig. 4). Based on the clustering patterns, which show a clear separation between groups, differences between the three environments were apparent and supported by Adonis analysis (*P*-values ranging from 0.001 to 0.028). Statistical differences between the three environments were further supported by ANOSIM and MRPP tests (on all detected genes: ANOSIM: $R = 0.786$, $P = 0.003$; MRPP: $\delta = 0.195$, $P = 0.007$). Likewise, significant differences were documented in the pairwise comparisons: active vs. non-active (Adonis *F*: 4.52, $P = 0.0001$, all detected genes) and active vs. microbially stabilized (Adonis *F*: 3.84, $P = 0.0001$, all detected genes). In contrast, lower statistical significance levels were documented for microbially stabilized vs. non-active communities (Adonis *F*: 2.59, $P = 0.058$, all detected genes).

Most of GEOCHIP 4.2 functional gene categories were present in our samples but their relative abundances varied. For instance, organic degradation and stress functional genes were highly enriched accounting for 16–25%, and 15–22.8% of all detected genes, respectively. Metal resistance genes recovered lower levels, ranging from 8.3 to 12.7%. Among the nutrient cycling genes, 9–13% were related to carbon utilization, of which 7–10% pertained to organic carbon degradation, whereas genes related to nitrogen cycling accounted for 5–7%, sulfur cycling: 2–3%, and phosphorus cycling: 1–2%.

Carbon cycling

All three environments were characterized by high levels of carbon fixation genes associated with autotrophic assimilation of CO_2 via the 3-hydroxypropionate cycle represented by propionyl-CoA/acetyl-CoA carboxylase (*pcc/acc*), and the Calvin–Benson CO_2 pathway represented by ribulose

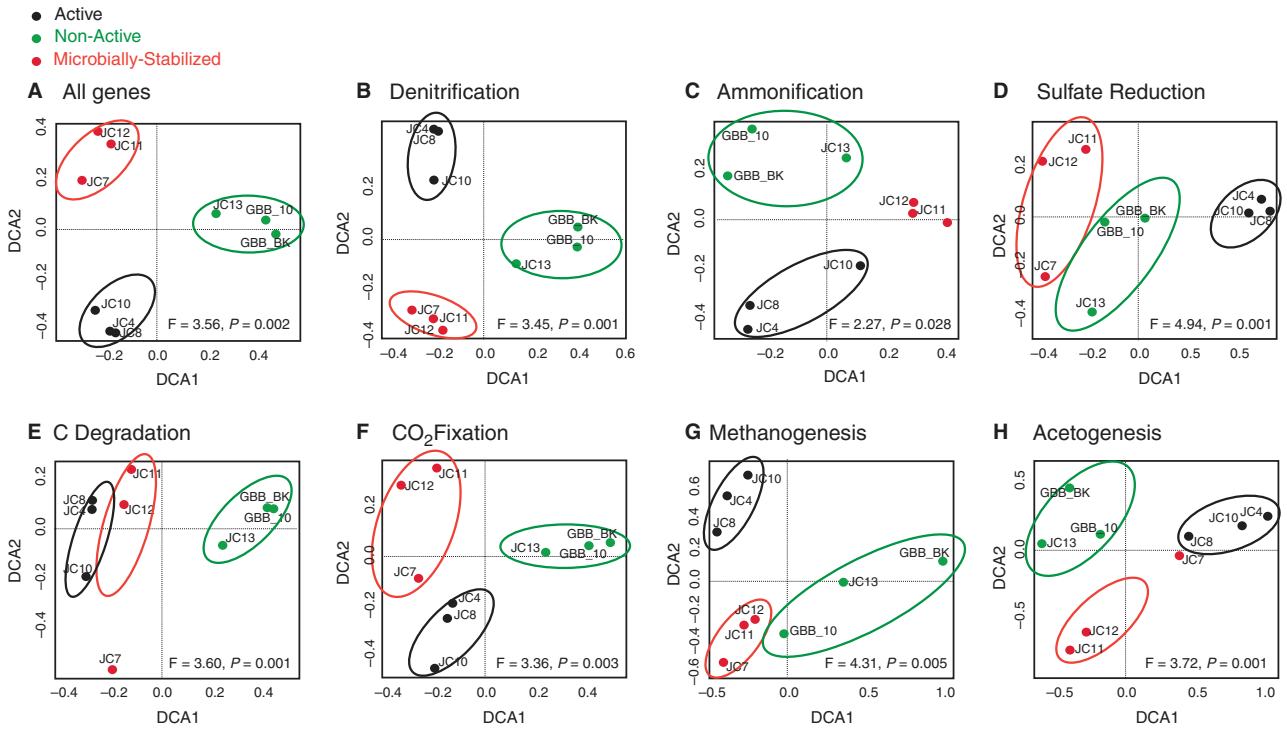

Fig. 4 Detrended correspondence analysis of various biogeochemical cycles based on hybridization signal intensities. (A) All genes within the array; (B) Denitrification; (C) Ammonification; (D) Sulfate reduction; (F) CO_2 fixation; (G) Methanogenesis; (H) Acetogenesis. Samples with the most similarity plot closer together, whereas samples with less similarity plot further apart. The dissimilarities were supported by Adonis analysis with *P*-values ranging from 0.028 to 0.001.

1,5-biphosphate carboxylase/oxygenase (RuBisCO). *Pcc/acc* was the most common, with abundance levels ~ threefold higher than RuBisCO (Fig. 5). While signal intensities associated with *pcc/acc* were found to differ between environmental pairwise comparisons (Adonis, $P = 0.001$), mat vs. non-active environments did not show significant differences (Adonis, $P = 0.073$). Over 45% and 32% of *pcc/acc* probes belonged to *Proteobacteria* and *Actinobacteria*, respectively (Fig. S1A). Other lineages included members within *Chloroflexi*, *Deinococcus-Thermus*, *Firmicutes*, *Bacteroidetes*, and *Euryarchaeota* lineages. Genes associated with RuBisCO were the second most abundant. While active environments recovered the lowest RuBisCO signal intensities, non-active environments recovered the highest. Among the three environments, active vs. mat communities showed the most significant differences (Adonis, $P = 0.001$). RuBisCO genes were mostly affiliated to *Proteobacteria* (*Alpha*, *Gamma*, *Beta*), and *Cyanobacteria* (Fig. S1B). Both phyla accounted for up to ~ 63% and 16% of the total number of RuBisCO probes, respectively, followed by representatives within *Firmicutes*, *Bacteroidetes*, *Chlorobi*, and *Thermotogae* lineages (Fig. S1B). Other autotrophic CO_2 fixation processes included the Wood–Ljungdahl pathway, represented by carbon monoxide dehydrogenase (CODH), and the reductive citric acid cycle, represented by ATP citrate lyase (*aclB-ATP)* (Fig. 5). The most significant differences in the level of abundance of CODH, which was the third most common type of autotrophic CO_2 fixation process, were observed between active and non-active communities (Adonis, $P = 0.001$) followed by active vs. mat environments (Adonis, $P = 0.023$). Most of CODH intensities were associated with *Proteobacteria* and included *Betaproteobacteria* (*Burkholderiales*) and *Alphaproteobacteria* lineages within *Rhizobiales*, *Rhodospirilalles*, *Rhodospirillum*, *Rhodobacterales* (Fig. S1C). Some species within *Rhizobiales, Rhodobacterales,* and *Burkholderiales* were solely present in microbially stabilized and/or non-active environments. Other CODH lineages included *Actinobacteria, Firmicutes,* and *Euryarchaeota*. In addition, all three environments were characterized by the presence of *aclB-ATP* and *bchY* genes, both of which are employed as biomarkers for anoxygenic phototrophs (Fig. 5). Except for *bchY* genes, which were found to exhibit significantly higher levels in non-active environments (non-active vs. mat: $P = 0.001$; non-active vs. active: $P = 0.001$; all based on Adonis), the *aclB-ATP* recovered similar signal levels with no statistical differences between environments. Taxonomic representatives of *aclB-ATP* included five distinct lineages, of which *Proteobacteria* and *Chlorobi* were the most abundant (Fig. S1D), whereas *bchY* genes were represented by four lineages with known aerobic anoxygenic or anoxygenic photosynthesizers within *Proteobacteria* (e.g., *Roseobacter* spp, *Rhodospirillum* spp.,

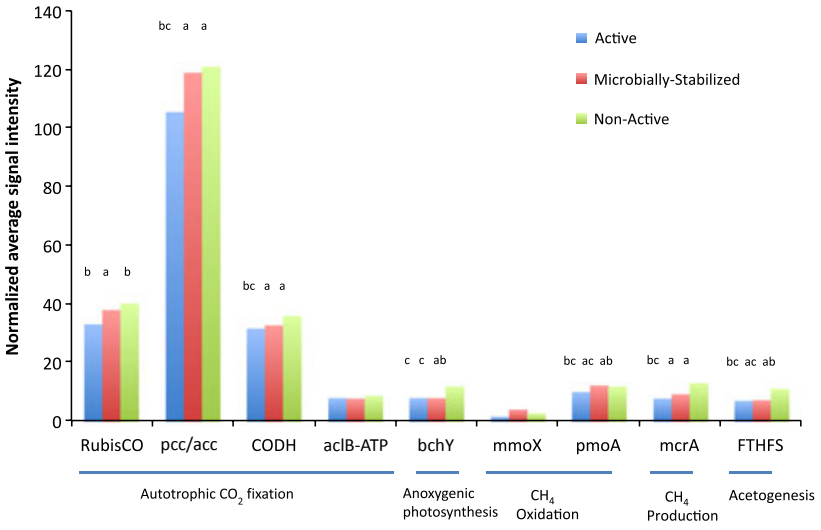

Fig. 5 Distribution of key gene families associated with carbon cycling. Autotrophic CO_2 fixation is represented by ribulose 1,5-biphosphate carboxylase/oxygenase (RuBisCO); propionyl-CoA/acetyl-CoA carboxylase (pcc/acc); carbon monoxide dehydrogenase (CODH); and ATP citrate lyase (*aclB-ATP*). Anoxygenic photosynthesis represented by bacteriochlorophyll Y (*bchY*). Methane oxidation includes methane monooxygenase (mmoX) and particulate methane monooxygenase (*pmoA*). Methane production is represented by methylcoenzyme M reductase (*mcrA*) and acetogenesis by formyltetrahydrofolate synthetase (FTHFS). The signal intensity for each functional gene is the average of the total signal intensity from all the replicates. Lowercase letters on top of each bar denote statistical significance between environmental categories (a = active, b = microbially stabilized, c = non-active) and functional genes ($P < 0.05$) by Adonis. Lack of letter indicates no statistical differentiation.

Erythrobacterium spp), *Cholorobi, Chloroflexus* and the purple sulfur bacterium, *Halorhodospira*.

Acetogenesis and methane metabolism

Genes indicative of acetogenesis (*FthFS*), methane production (*mcrA*), and methane oxidation (*mmox, pmoA*) were present and exhibited signal intensities which were ~fivefold to 12-fold lower than autotrophic CO_2 fixation genes (Fig. 5). Acetogenesis was represented by four distinct lineages, representing the genera *Rubrobacter, Clostridium, Norcadiodes, Corynebacterium, Shewanella*, and *Lactobacillus,* some of which were solely present in mat stabilized/and or non-active environments (Fig. S2A, B). Gene sequences associated with aerobic type I-II methanotrophs, for example, *Methylomicrobium, Methylocapsa, Methylocystis, Norcadiodes,* were recovered in all three environments, except for *Methylomicrobium*, which was only present in microbially stabilized environments (Fig. S2C,D). Methanogens occurred in low numbers in all three environments and were mostly affiliated to uncultured *Archaea* and few isolates belonging to *Methanocorpusculum* and *Methanococcus*.

Carbon degradation

Carbon degradation genes were highly enriched and surpassed those involved in carbon fixation processes. The most labile forms of carbon, for example, starch, hemicellulose, and cellulose, recovered a wider array of enzymes than recalcitrant compounds, for example, aromatics, chitin, lignin, and pectin (Fig. 6). Although all three environments documented high signal intensities for amylase (starch), endochitinase (chitin), ara (hemicellulose), and acetylglucosaminidase (chitin), active environments recovered lower intensities, except for cda (starch), which displayed higher signals in microbially stabilized environments. Carbon degradation genes were mostly affiliated to bacteria, representing 65.3% of the total pool of carbon degrading genes, whereas fungi-associated genes (e.g., *Ascomycota* and *Basidiomycota*) contributed 33.4%. Other minor contributors included members within the *Archaea* (e.g., *Euryarchaeota* and *Crenarchaeota*).

Nitrogen cycling

Five different enzymes involved in denitrification including nitrate reductase (narG), nitrite reductase (*nirK, nirS*), nitric oxide reductase (*norB*), and nitrous oxide reductase (*nosZ*) were documented (Fig. 7). All three environments significantly differed in the signal strength of *nirK* (Adonis, $P = 0.001$, all pairwise comparisons), *nirS* (Adonis, $P = 0.001$, all pairwise comparisons), and *narG* (Adonis, $P = 0.050$–0.032). While *nosZ* gene signals were found to differ among active vs. microbially stabilized (Adonis, $P = 0.008$) and between non-active and microbially stabilized environments (Adonis, $P = 0.017$), *norB* signals only exhibited significant differences between active and microbially stabilized environments (Adonis, $P = 0.017$). When pooling all five functional genes, the signal intensities were significantly different (Adonis, $P = 0.001$), with higher levels documented for non-active and microbially stabilized

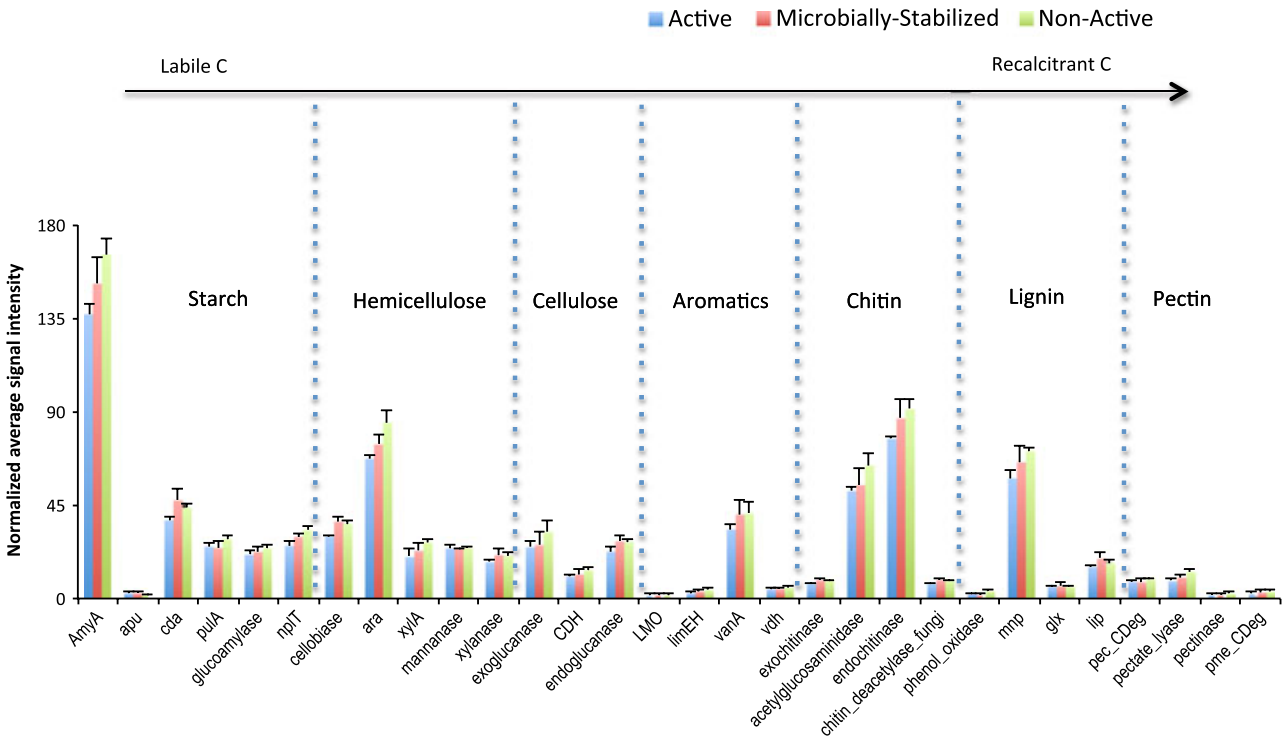

Fig. 6 Genes involved in carbon degradation. Genes arranged based on the complexity of carbon from labile to recalcitrant. The signal intensity for each function gene is the average of the total signal intensity from all replicates. Error bars denote standard deviation. Abbreviations denote: *AmylA* (alpha amylase); *apu* (*amyX*/*pullanase*); *cda* (cyclo- maltodextrin dextrin-hydrolase); *pulA* (pullanase); *nplT* (neopullulanase); *ara* (arabinose); *xylA* (xylose isomerase); *CDH* (cellobiose dehydrogenase); *LMO* (lignin-modifying oxidase); *limEH* (limonene-1,2-epoxide hydrolase); *vanA* (vanillate monooxygenase); *vdh* (vanillin dehydrogenase); *mnp* (manganese peroxidase); *glx* (glyoxal oxidase); *lip* (ligninase); *pec*_Cdeg (pectinase degradation); *pme*_Cdeg (pectin methylesterase).

environments. Whereas the vast majority of denitrification genes were related to uncultured denitrifrying bacteria, up to 57% of the identified genes represented denitrifiers from *Beta* (*Burkholderiales)*, *Alpha* (*Rhizobiales, Rhodobacterales*), and *Gammaproteobacteria* (*Enterobacteriales*, *Pseudomonadales*) (Fig. S3A,B). *Ascomycota* (*Eurotiomycetes, Sordariomycetes*) represented the second most abundant group comprising up to 35% of the identified denitrifiers lineages. Other less representative groups included *Euryarchaeota*, *Firmicutes*, *Verrucomicrobia*, and *Aquificeae*. Among these, the *Aquificeae* lineage was only present in non-active communities. Besides genes involved in denitrification, which recovered seven phyla, GEOCHIP 4.2 detected two key enzymes involved in ammonification processes, for example,. glutamate dehydrogenase (*gdh*) and urease c (*ureC*). Based on hybridization signal strengths, ammonification is mostly represented by *ureC* genes (Fig. 7). Except for non-active vs. microbially stabilized environments, which showed $P = 0.022$ (Adonis), all other environments showed differences at $P = 0.001$ (Adonis) in *ureC* genes. Ninety-eight percent of the ammonification genes (e.g., *gdh, ureC*) were associated with established species within nine different phyla. *Proteobacteria* (*Alpha*, *Gamma*, *Beta*) represented over 50% of the detected genes followed by *Actinobacteria* (up to 27%) and *Cyanobacteria* (up to 8%) (Fig. S4).

Functional genes related to N_2 fixation were also documented and based on intensity levels the *nif*H gene ranked as the most abundant gene (Fig. 7). As with *nirK* and *nirS*, significant differences in the total signal intensity of *nifH* genes were observed among all sites (Adonis, $P = 0.001$, all pairwise comparisons) with higher levels documented in non-active and microbially stabilized environments. Although an overwhelming majority of *nifH* genes (72%) was from uncultured organisms, eight different phyla were identified, among which, *Cyanobacteria*, *Proteobacteria*, *Eurychaeota*, and *Firmicutes* accounted for most of the *nifH* genes (Fig. S5A,B).

Genes associated with anaerobic ammonium oxidation (anammox, *hzo*) and nitrification (*hao*) were present at relatively low levels (Fig. 7). Signals related to *hzo* were associated with uncultured *Planctomycetes*. Likewise, *hao* signals were mostly related to uncultured *Planctomycetes* and to *Nitrosomonas* sp NM 143 and *Candidatus Kuenenia stuttgartiensis,* both with capability for nitrification.

Sulfur cycling genes

Most key functional genes involved in sulfur cycling were detected (Fig. 8). Genes related to sulfite reductase (e.g.,

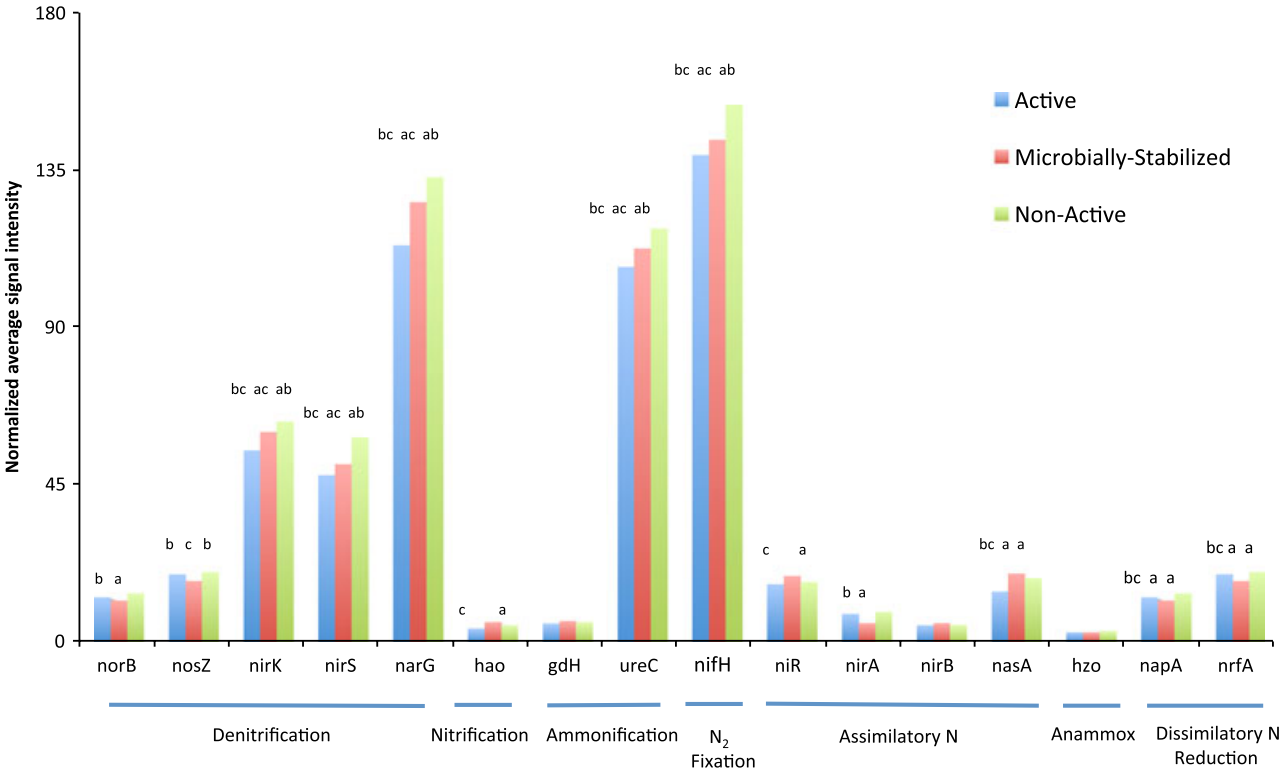

Fig. 7 Normalized signal intensity of genes involved in nitrogen cycling. Abbreviations denote *norB* (nitric oxide reductase); *nosZ* (nitrous oxide reductase); *nirK/nirS* (nitrite reductases); *narG* (nitrate reductase); *hao* (hydroxylamine oxidoreductase); *gdh* (glutamate dehydrogenase); *ureC* (urease); *nifH* (nitrogenase); *niR/nirA/nirB* (nitrite reductases); nasA (nitrate reductase); *hzo* (hydrazine oxido-reductase); *napA* (nitrate reductase periplasmic); *nrfA* (nitrite reductase). The signal intensity for each functional gene is the average of the total signal intensity from all the replicates. Lowercase letters on top of each bar denote statistical significance between environmental categories (a = active, b = microbially stabilized, c = non-active) and functional genes ($P < 0.05$) by Adonis. Lack of letter indicates no statistical differentiation.

dsrA/B, *cysJ/I*) and sulfur oxidation (e.g., *sox)* were most abundant, whereas genes related to sulfide oxidation (e.g., *sqR*, *fccAB*) were less abundant. As previously documented, active environments consistently displayed lower signal intensities as opposed to mat and non-active environments. When combining all sulfite reduction genes, Adonis tests revealed significant differences between pairwise comparisons of active vs. mat ($P = 0.001$) and active vs. non-active ($P = 0.009$). In contrast, no significant differences were documented between non-active and mat communities. Dissimilatory sulfite reductase genes (*dsrA/B*) were the most prevalent, accounting for over 45% of the sulfur genes. Most *dsrA/B* genes (~78%) were associated with uncultured sulfate-reducing bacteria. Among the identified lineages, up to 31.8% belonged to *Deltaproteobacteria* (e.g., *Desulfobacterales, Desulfovibrionales*), whereas *Firmicutes* (e.g., *Clostridiales*) accounted for up to 29.5% of *dsrA/B* genes (Fig. S6A, B). Assimilatory sulfite reductase genes, for example, *CysJ/I*, *sir*, represented 22% of the total sulfur genes. While 41% of the *CysJ/I* genes belonged to *Gammaproteobacteria*, 55% of the *sir* genes were related to *Cyanobacteria* and *Gammaproteobacteria* (data not shown). Sulfur oxidation recovered a total of 65 *sox* genes, most of which were associated with *Alphaproteobacteia* (*Rhodobacteraceae*, *Rhizobiales*) and *Gammaproteobacteria* (*Chromatiales*). Other less representative members included *Chlorobi* (*Chlorobiales)* and *Betaproteobacteria* (*Burkholderiales*).

Extracellular polymeric substance determinations

Extracellular polymeric substance determinations, as established by phenol-sulfuric acid quantification, showed that microbially stabilized EPS content was ~10- to 3.8-fold higher than active and non-active samples, respectively (Fig. 9). In contrast, non-active samples displayed EPS concentrations, which were on average ~threefold higher than active communities. The differences in EPS content were statistically well supported by *t*-test analysis with *P*-values ranging from 0.002 to 0.003.

While the distribution of EPS in active and non-active samples recovered at different localities (e.g., Shroud Cay and Joulters Cay) did not appear to be significantly different from each other, EPS on mat-associated oolitic grains significantly differ at both localities (*t*-test, $P = 0.05$), with higher levels documented in Shroud Cay and surpassing over 52%

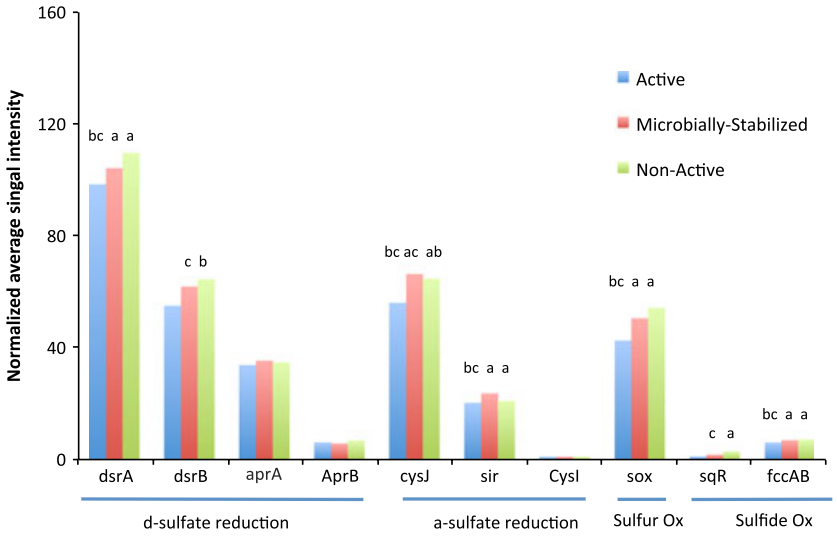

Fig. 8 Normalized signal intensity of genes involved in sulfur cycling. Abbreviations denote: *dsrA/dsrB* (sulfite reduction); *aprA/AprB* (dissimilatory adenosine 5′-phosposulfate reductases); *CysJ/CysI/sir* (sulfite reductases); *sox* (sulfite oxidase); *sqR* (sulfide quinone reductase); *fccAB* (flavocytochrome c sulfide dehydrogenase). The signal intensity for each functional gene is the average of the total signal intensity from all the replicates. Lowercase letters on top of each bar denote statistical significance between environmental categories (a = active, b = microbially stabilized, c = non-active) and functional genes ($P < 0.05$) by Adonis. Lack of letter indicates no statistical differentiation.

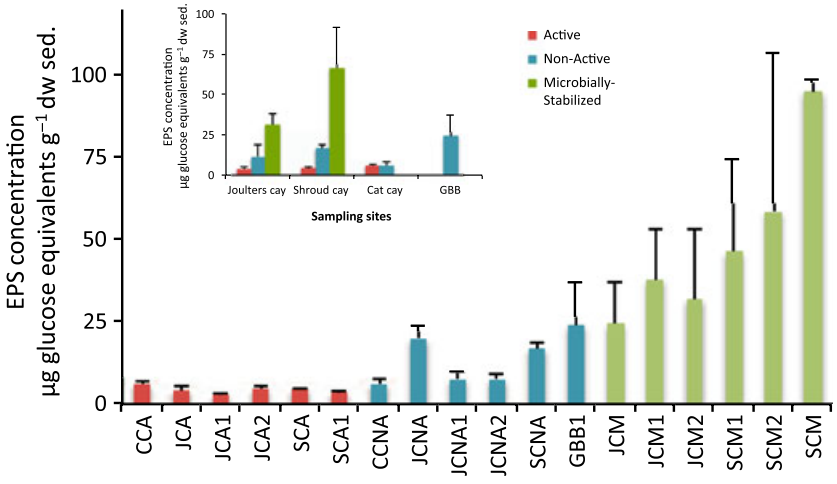

Fig. 9 Distribution of extracellular polymeric substance (EPS) content at different locations. Inset graph represents pooled data of environmental sites. EPS concentrations are based on phenol-sulfuric acid quantification. Concentrations of EPS are given as µg of glucose equivalents per gram of dry weight. Error bars represent the standard deviation of three sets of samples per environment (for each set $n = 2$).

those of Joulters Cay (Fig. 9). Similarly, significant differences (*t*-test, P = 0.03) were documented between non-active samples from Shroud Cay and Cat Cay. Further differences were also established between active sampling sites: 1) Cat Cay vs. Shroud Cay (*t*-test, $P = 0.045$) and 2) Cat Cay vs. Joulters Cay (*t*-test, $P = 0.040$).

DISCUSSION

Oolitic carbonate sediments of the Bahamas Archipelago harbor diverse microbial communities with metabolic potential for major biogeochemical processes (Fig. 10). Based on functional diversity indices, non-active communities are the most diverse, followed by microbially stabilized and active environments. This is in agreement with Diaz *et al.* (2013), who documented a similar diversity trend using clone libraries of the 16S rRNA gene in the oolitic sediments of the Bahamas. The average Shannon–Weaver functional diversity index [H = 9.14], although lower than in the mangrove sediments from South China [average: H = 10.22] (Bai *et al.*, 2012), surpasses the levels reported by others using similar technology in the sediments from the Gulf of Mexico [average: H = 5.23] (Wu *et al.*, 2008) and Juan de Fuca hydrothermal vents [average: H = 5.75] (Wang *et al.*, 2009). The high level of microbial diversity may be created by physical disturbances (e.g., tides, currents), which can induce spatial and temporal heterogeneity, allowing for the creation of new niches to support diverse microbial assemblages (Ley *et al.*, 2006).

Despite established dissimilarities, which were mostly driven by gene abundance and phylogenetic composition, microbial oolitic communities shared extensive phylogenetic and functional gene overlap, which might be indicative of functional redundancy that allows these communities to persist under different levels of physical disturbances and environmental conditions. In spite of functional redundancy, significant variability of functional genes related to carbon, nitrogen, and sulfur cycling was

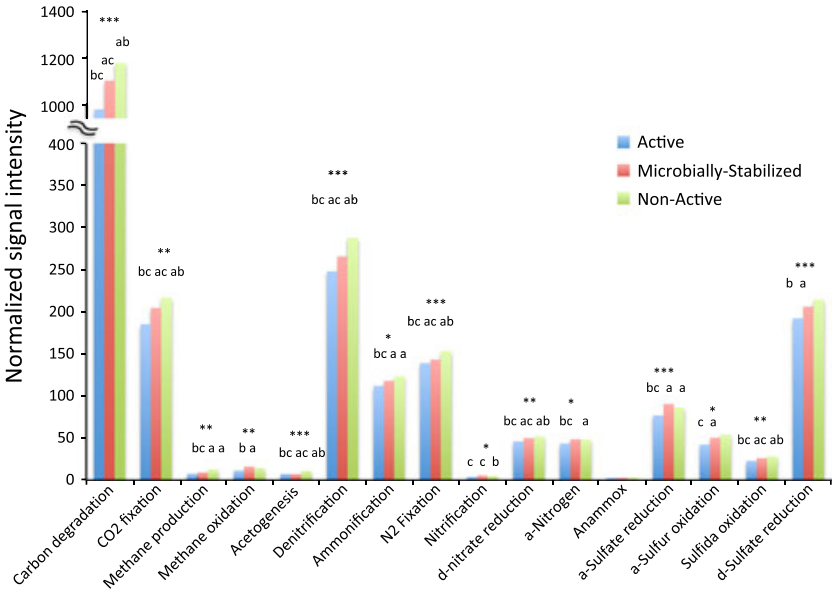

Fig. 10 Summary of metabolic processes associated with oolitic microbial communities. The normalized signal intensity is the average of the total signal intensity from all the replicates associated with individual metabolic process. Lowercase letters on top of each bar denote statistical significance between environmental categories (a = active, b = microbially stabilized, c = non-active) and functional genes ($P < 0.05$) by Adonis. Lack of letter indicates no statistical differentiation. Asterisks denotes global statistical significance among all pairwise comparisons based on Adonis analysis ***$P < 0.0001$, **$P < 0.001$, *$P < 0.05$.

evident. Although we could not be certain about the main factor contributing to the documented differences as environmental variables were not assessed, we speculate contrasting hydrodynamic flows, which ranges from 100 cm s^{-1} in active environments to 2 cm s^{-1} in stabilized areas (Smith, 1995; Rankey *et al.*, 2006), could account for some of the differences. For instance, hydrodynamic forces are known to impact bacterial community structure and function as they can affect the sediments redox conditions (Mills *et al.*, 2008).

While assemblages of *Proteobacteria* exhibiting a wide range of metabolic pathways have the potential to promote degradation and remineralization within all three environments, bacterial primary production in ooid environments seems to be driven by a diverse population of autotrophic CO_2 fixers, among which *Proteobacteria (Alpha-Beta, Gamma)*, *Chlorobi*, and *Cyanobacteria* are the most prevalent. These findings are supported by Diaz *et al.* (2013), who documented similar taxonomic composition of primary producers in oolitic sediments from the Bahamas using terminal fragment length polymorphism (TRFLPs) and 16S rRNA clone analysis. Based on the ubiquitous presence of both oxygenic and anoxygenic phototrophs, all of which can drive the alkalinity toward carbonate precipitation by consuming CO_2 and increasing local pH (Bosak *et al.*, 2007; Dupraz *et al.*, 2009), we can infer these communities could have metabolic capabilities for carbonate precipitation as documented in systems, such as microbialites (Breitbart *et al.*, 2009); stromatolites (Dupraz & Visscher, 2005); and fresh-water ooids (Pacton *et al.*, 2012). Functional gene analysis unveiled a large number of genes for CO_2 fixation through the 3-hydroxypropionate/malyl CoA cycle (*pcc/acc*), the Calvin–Benson (RuBisCO), and the Wood–Ljungdahl pathway (CODH). Abundance of *pcc/acc* over RuBisCO was surprising as primary production in marine photic zones is generally attributed to autotrophic organisms (e.g., cyanobacteria and eukaryotic algae) that employ RuBisCO as the CO_2 fixation mechanism (Hügler & Sievert, 2011). In contrast, 3-hydroxypropionate/malyl CoA cycle is a more restricted cycle, mostly circumscribed to *Chloroflexaceae* (Strauss & Fuchs, 1993; Zarzycki *et al.*, 2009), members within *Alpha-* (*Erythrobacter* spp.), *Gamma-* (NOR5-3, NOR51-B), and autotrophic archaea (Zarzycki *et al.*, 2009). Although this metabolic pathway is probably more common than previously thought, the predominance of *pcc/acc* in oolitic sediments should be regarded with caution as this pathway comprises a heterogeneous group of multifunctional carboxylating enzymes (Lombard & Moreira, 2011). The Wood–Ljungdahl pathway was the third most common CO_2 fixation mechanism. Although this pathway is mostly circumscribed to anaerobes that couple CO oxidation to sulfate reduction or reduce CO_2 to either acetate or methane (Hügler & Sievert, 2011), 61% of the probes targeted aerobic carboxydotrophs (e.g., *Rhizobiales, Rhodobacterales, Actinobacteria*) capable of oxidizing CO to CO_2 (Lorite *et al.*, 2000; King & Weber, 2007; Park *et al.*, 2008). Other autotrophic fixation mechanism, include the reverse tricarboxylic acid (rTCA) cycle, which was mostly represented by *Chlorobium limicola* and few microaerophilic members within *Proteobacteria* and *Aquificales*, has been previously documented in marine microbial communities (Campbell & Cary, 2004).

GEOCHIP analysis identified carbon degradation as one of the most abundant gene categories in the carbon cycling with signal intensities ~fivefold higher than autotrophic CO_2 fixation (Fig. 10). The widespread array of genes associated with organic carbon substrates suggests these heterotrophic communities have a high plasticity in meta-

bolic pathways that enables them to degrade simple and complex carbohydrates and exploit limited carbon sources, which are commonly associated with oligotrophic waters. For instance, the ability of marine microbes to use labile and recalcitrant organic matter (e.g., chitin, cellulose, and lignin) as carbon, nitrogen, and energy sources has been documented by others (Sieburth, 1976; Bianchi, 2011). While the vast majority of heterotrophic metabolism in oolitic environments seems to be regulated by bacteria, a third was associated with fungal communities (e.g., *Ascomycota* and *Basidiomycota*) with potential capabilities for degradation of large organic polymers (e.g., chitin, lignin, pectin). The occurrence of fungal communities, which was further validated by PCRs of the LSU rRNA gene with panfungal primers, for example, F63 and R635 (unpublished data), is not unforeseen as endolithic fungi has been previously documented in ooids (Kahle, 1977; Harris *et al.*, 1979; Gerdes & Krumbein, 1987). Although their significance has yet to be established, these communities can have potential capacities to exploit mineralized organic matter entrapped in carbonate substrates (Golubic *et al.*, 2005). Herein, we also documented carbon cycling processes, which are indicative of acetogenesis and C1 pathways (e.g., methanogenesis, methane oxidation), but based on the signal intensities, they do not seem relevant pathways (Fig. 10).

The nitrogen cycle, which is driven by complex biogeochemical transformations that include denitrification, N_2 fixation, ammonification, and assimilation, is considered one of the most important biogeochemical cycles as it controls the productivity of the oceans (Zehr & Kudela, 2011). Our results revealed a wide variety of functional genes with different degrees of abundance for processes involved in nitrogen cycling. Based on the abundance and levels of intensity of nitrogen-related genes, denitrification seems an important biogeochemical process, mostly driven by uncultured organisms and members within *Proteobacteria* lineages (e.g., *Pseudomonas*, etc). This finding supports previous studies documenting the presence of denitrifying communities in oolitic environments (Diaz *et al.*, 2013). In addition, denitrifying communities (e.g., *Pseudomonas*, etc) have been implicated in the chalky mud flat precipitation in the Bahamas (Drew, 1911, 1914). N_2 fixation genes, which were the second most abundant nitrogen-related gene family, followed by ammonification, identified lineages associated with *Euryarchaeota, Proteobacteria*, and *Cyanobacteria,* suggesting these communities may have an important role as contributors to nitrogen in these nitrate-poor oligotrophic Bahamian waters (Karl *et al.*, 2002). However, further validation is needed to assess the activity of these genes and associated communities. Likewise, ammonification seems a relevant pathway as *ureC* gene, which is a functional marker for urea utilization potential, ranked as third. Urea is considered a predominant nitrogen source in oligotrophic oceans, where regenerated forms of nitrogen (e.g., urea and ammonium) are the preferred nitrogen source of many organisms (Antia *et al.*, 1991). Hydrolysis of urea can generate carbonate alkalinity, which can promote precipitation. Based on GEOCHIP 4.2, urea utilizers were abundant and include diverse phylo-groups, mostly represented by *Proteobacteria* and *Actinobacteria*. In contrast, the level of detection of genes for nitrification and anammox processes was relatively low. Similar findings have been reported for thrombolites in the Bahamas (Mobberley *et al.*, 2013) and microbialites from Cuatro Ciénaga, Mexico (Breitbart *et al.*, 2009).

The microbial communities in these oolitic sediments appear to be capable of a variety of S cycling processes, and based on gene abundance levels, sulfate reduction recovered the highest number of S-related genes followed by sulfur oxidation and sulfide oxidation. Sulfate reduction can account for over 50% of the organic carbon mineralization in marine sediments and provide a source of electrons to phototrophic and chemolithotrophic bacteria (Jørgensen, 1982). This important metabolic process generates carbonate ions, which can potentially lead to calcium precipitation (Decho *et al.*, 2005; Dupraz & Visscher, 2005). Although sulfate reduction genes were associated with well-established sulfate-reducing genera within *Deltaproteobacteria* and *Firmicutes* (i.e., *Desulfovibrio, Syntrophobacter, Desulfotomaculum, Clostridium*), the vast majority of sulfate reduction genes were from uncultured clones, indicating that major uncultured diversity lies in these environments. Similar findings applied for denitrifiers, with only 13% of the genes characterized. The presence of denitrifiers and sulfate reducers in active ooid sediments, which was previously documented by Diaz *et al.* (2013) in the oolitic environments in the Bahamas Archipelago, suggests these organisms, which were previously thought restricted to anoxic environments, can tolerate oxic conditions (Krekeler *et al.*, 1998; Sigalevich *et al.*, 2000; Baumgartner *et al.*, 2006; Hunter *et al.*, 2006; Gao *et al.*, 2010; Wang *et al.*, 2011b). For instance, high rates of aerobic denitrification have been reported in sandy sediments exposed to tidally induced redox oscillations (Gao *et al.*, 2010; Wang *et al.*, 2011b). Similarly, a highly active population of sulfate reducers has been documented in the oxic zones of stromatolite systems in the Bahamas (Visscher *et al.*, 2000; Dupraz *et al.*, 2004) and in the hypersaline mats at Guerrero Negro, Mexico (Canfield & Des Marais, 1991). These organisms, which bear oxidative defense mechanisms that can counteract free radicals, can even exhibit higher rates of sulfate reduction under oxic conditions (Canfield & Des Marais, 1991; Fournier *et al.*, 2004; Baumgartner *et al.*, 2006; Bryukhanov *et al.*, 2011). Based on our GEOCHIP 4.2 data, all three environments recovered a number of genes associated with oxidative stress resistance mechanisms, including oxidoreductases (e.g., ferredoxin: NADPH

(FNR), catalases (e.g., *katA/E*), and hydroperoxidases (e.g., *AhpC/F*, *OxyR*) (data not shown). In addition, we detected genes associated with hydrogen peroxide detoxification (e.g., *cydA/B*) (Lindqvist *et al.*, 2000). Besides the aforementioned mechanisms against reactive oxygen species, particle-attached biofilms could further promote oxygen-depleted microniches (Kuhl & Jorgensen, 1992). According to Diaz *et al.* (2013), oolitic communities are characterized by the ubiquitous presence of particle-attached bacteria and EPS producers/degraders (e.g., sulfate reducers and lineages within *Proteobacteria*, *Planctomycetes, Bacteroidetes, Cyanobacteria*), all of which can combine to create steep redox gradients to facilitate anaerobic metabolism in an otherwise oxygenated environment (Paerl & Prufert, 1987). A similar mechanism has been reported for microbialite systems, where copious amount of EPS secreted by micro-organisms (e.g., sulfate reducers, cyanobacteria) induce steep/redox gradients (Breitbart *et al.*, 2009).

Measurements of EPS abundance associated with oolitic grains provide further evidence for the ubiquitous presence of EPS biofilm and associated communities. Our results, which showed a gradual increase in EPS concentration from active to mat stabilized environments, suggests that hydrodynamic forces can have a direct effect on EPS accumulation. Thus, lower abundance of EPS (4 μg glucose equivalents g^{-1} dw sed.) on active oolitic grains is probably due to shear forces that promote detachment of EPS (Zhang *et al.*, 2011; Piggot *et al.*, 2012; Diaz *et al.*, 2013), whereas stabilized areas allow for more EPS accumulation with average values ranging from 13.6 to 49 glucose equivalents g^{-1} dw sed. for non-active and microbially stabilized environments, respectively. Our documented EPS levels are in agreement with Diaz *et al.* (2013), who documented EPS levels ranging from 11.6 to 31.4 μg glucose equivalents g^{-1} dw sed. on oolitic grains in Joulters Cays. The role of EPS in calcium carbonate precipitation has been extensively studied in various microbial systems, for example, stromatolites, microbialites, and dolomites (Decho, 2000; Decho *et al.*, 2003; Dupraz & Visscher, 2005), and has revealed that heterotrophic bacteria, including sulfate reducer bacteria, play an important role in the gross calcification via release of Ca^{2+} ions formerly bound to acidic EPS groups.

Even though GEOCHIP 4.2 has its limitations (as it measures potential rather than 'actual' microbial activities and suffers from lack of resolution at detecting novel gene sequences), this study provides a comprehensive snapshot on gene diversity, distribution, and putative metabolic capabilities of these understudied microbial communities. Nevertheless, further studies are warranted using mRNA analysis to establish a more direct link between microbial communities and functional activities and how their metabolic activities and physo-chemical conditions of the environment can influence carbonate precipitation.

CONCLUSIONS AND IMPLICATIONS

Functional gene diversity in oolitic environments is relatively high, with higher diversity associated with non-active and microbially stabilized environments. Despite differences in overall microbial community structure, oolitic microbial communities share functional redundancy for metabolic processes that potentially fosters carbonate precipitation. The latter is supported by the co-occurrence and abundance of genes associated with photosynthesis, denitrification, ammonification, and sulfate reduction (Fig. 10). Except for organic carbon degradation, most of the processes associated with carbonate dissolution (e.g., sulfide oxidation, methane oxidation, ammonium oxidation, dissimilatory nitrate reduction) do not seem as predominant. EPS analysis along with functional gene analysis, which revealed genes encoding EPS-degrading enzymes (chitinases, glucoamylase, amylases), further supports the putative role of EPS degraders in calcification. While recent studies attribute photosynthesizers as the primary drivers for the genesis of freshwater ooids (Plée *et al.*, 2008, 2010; Pacton *et al.*, 2012) and calcification processes in hypersaline mats in lake Chiprana, Spain (Ludwig *et al.*, 2005), there is circumstantial evidence to speculate that $CaCO_3$ precipitation in oolitic environments is probably biologically influenced by the synergistic effect of microbes with diverse physiologies (e.g., oxygenic/anoxygenic photoautotrophs, oxygenic/anoxygenic heterotrophs, denitrifiers, sulfate reducers, ammonifiers). This is further supported by Diaz *et al.* (2013), who documented the occurrence of key phylogenetic groups with capability for $CaCO_3$ precipitation in Bahamian ooids and by lipid biomarker signatures of sulfate-reducing bacteria, photoautotrophs, and heterotrophs in the oolitic sands of the Bahamas and Shark Bay, Australia (Summons *et al.*, 2013). The integration and coordination of metabolic processes that favors precipitation or dissolution along the spatially distinct microenvironments further induced by EPS biofilm can possibly mediate carbonate precipitation in this otherwise oxygen and carbonate-saturated environment.

ACKNOWLEDGEMENTS

The authors wish to thank A. Oehlert, K. Jackson, and P. Harris for sampling collection; T. Yuan for valuable laboratory assistance; and Y. Deng for bioinformatics assistance. This work was supported by funds from the Industrial Associates of the University of Miami Center for Carbonate Research (CSL).

REFERENCES

Antia NJ, Harrison PJ, Oliveira L (1991) The role of dissolved organic nitrogen in phytoplankton nutrition, cell biology and ecology. *Phycologia* **30**, 1–89.

Antonov JI, Locarnini RA, Boyer TP, Mishonov AV, Garcia HE (2006) World Ocean Atlas 2005. In *Volume 2: Salinity. NOAA Atlas NESDIS 62* (ed. Levitus S). US Government Printing Office, Washington, DC, pp. 182.

Bai S, Li J, He Z, Van Norstrand JD, Tian Y, Lin G, Zhou J, Zheng T (2012) GeoChip-based analysis of the functional gene diversity and metabolic potential of soil microbial communities of mangroves. *Applied Microbiology and Biotechnology* **97**, 7035–7048.

Ball MM (1967) Carbonate sand bodies of Florida and the Bahamas. *Journal of Sedimentary Petrology* **37**, 556–591.

Baumgartner LK, Reid RP, Dupraz C, Decho AW, Buckley DH, Spear JR, Przekop KM, Visscher PT (2006) Sulfate reducing bacteria in microbial mats: changing paradigms, new discoveries. *Sedimentary Geology* **185**, 131–145.

Benson DJ (1988) Depositional history of the smackover formation in southwest Alabama Gulf Coast. *Gulf Coast Association of Geological Societies Transactions* **38**, 197–205.

Bianchi TS (2011) The role of terrestrially derived organic carbon in the coastal ocean: A changing paradigm and the priming effect. *Proceeding of the National Academy of Sciences of the USA* **108**, 19473–19481.

Bosak T, Greene SE, Newman DK (2007) A likely role for anoxygenic photosynthetic microbes in the formation of ancient stromatolites. *Geobiology* **5**, 119–126.

Braissant O, Decho AW, Przekop KM, Gallagher KM, Glunk C, Dupraz C, Visscher PT (2009) Characteristics and turnover of exopolymeric substances (EPS) in a hypersaline microbial mat. *FEMS Microbiology Letters* **67**, 293–307.

Breitbart M, Hoare A, Nitti A, Haynes M, Dinsdale E, Edwards R, Souza V, Rohwer F, Hollander D (2009) Metagenomic and stable isotopic analyses of modern freshwater microbialites in Cuatro Ciénegas, Mexico. *Environmental Microbiology* **11**, 16–34.

Bryukhanov AL, Korneeva VA, Kanapatskii TA, Zakharova EE, Men'ko EV, Rusanov II, Pimenov NV (2011) Investigation of the sulfate reducing bacterial community in the aerobic water and chemocline zone of the Black Sea by the Fish technique. *Microbiology* **80**, 108–116.

Campbell BJ, Cary SC (2004) Abundance of reverse tricarboxylic acid cycle genes in free-living microorganisms at deep-sea hydrothermal vents. *Applied and Environmental Microbiology* **70**, 6282–6289.

Canfield DE, Des Marais DJ (1991) Aerobic sulfate reduction in microbial mats. *Science* **251**, 1471–1473.

Castanier S, Le Métayer-Levrel G, Perthuisot JP (2000) Bacterial roles in the precipitation of carbonate minerals. In *Microbial Sediments* (eds Riding RE, Awramik SM). Springer-Verlag, Heidelberg, pp. 32–39.

Chan Y, Van Nostrand JD, Zhou J, Pointing S, Farrell RL (2013) Functional ecology of an Antartic Dry Valley. *Proceeding of the National Academy of Sciences of the USA* **110**, 8990–8995.

Cruz FEG (2008) Processes, patterns and petrophysical heterogeneity of grainstone shoals at Ocean Cay, Western Great Bahama Bank. Ph.D. dissertation, University of Miami, Miami, FL, pp. 163.

Davey ME, O'Toole GA (2000) Microbial biofilms: from ecology to molecular genetics. *Microbiology and Molecular Biology Reviews* **64**, 847–867.

Davies GR (1970) Carbonate bank sedimentation, eastern Shark Bay, Western Australia. In *Carbonate Sedimentation and Environments, Shark Bay, Western Australia* (eds. Logan BW, Davies GR, Read JF, Cebulski E). AAPG Memoir 13, Tulsa, OK, pp. 85–168.

Davies PJ, Bubela B, Ferguson J (1978) The formation of ooids. *Sedimentology* **25**, 703–730.

Decho AW (1990) Microbial exopolymer secretions in ocean environments: their role(s) in food webs and marine processes. *Oceanography and Marine Biology: An Annual Review* **28**, 73–153.

Decho AW (2000) Exopolymer microdomains as a structuring agent for heterogeneity within microbial biofilms. In *Microbial Sediments* (eds Riding RE, Awramik SM). Springer-Verlag, Berlin, Germany, pp. 1–9.

Decho AW, Kawaguchi T, Allison MA, Louchard EM, Reid RP, Stephens FC, Voss KJ, Wheatcroft RA, Taylor BB (2003) Sediment properties influencing upwelling spectral reflectance signatures: The biofilm gel effect. *Limnology and Oceanography* **48**, 431–443.

Decho AW, Visscher PT, Reid P (2005) Production and cycling of natural microbial exopolymers (EPS) within a marine stromatolite. *Palaeogeography and Palaeoclimatology* **219**, 71–86.

Diaz MR, Piggot A, Eberli GP, Klaus JS (2013) Bacterial community of oolitic carbonate sediments of the Bahamas Archipielago. *Marine Ecology Progress Series* **485**, 9–24.

Drew GH (1911) The action of some denitrifying bacteria in tropical and temperate seas and the bacterial precipitation of calcium carbonate in the sea. *Journal of the Marine Biological Association* **9**, 142–155.

Drew GH (1914) On the precipitation of calcium carbonate by marine bacteria and on the action of denitrifying bacteria in tropical and temperate seas. *Papers from the Tortugas Laboratory of the Carnegie Institution of Washington* **5**, 7–45.

Duguid SMA, Keyser TK, James NP, Rankey EC (2010) Microbes and ooids. *Journal of Sedimentary Research* **80**, 236–251.

Dupraz C, Visscher PT (2005) Microbial lithification in marine stromatolites and hypersaline mats. *Trends in Microbiology* **13**, 429–438.

Dupraz C, Visscher PT, Baumgartner LK, Reid RP (2004) Microbe-mineral interactions: early carbonate precipitation in a hypersaline lake (Eleuthera Island, Bahamas). *Sedimentology* **51**, 745–765.

Dupraz C, Reid RP, Braissant O, Decho AW, Norman RS, Visscher PT (2009) Processes of carbonate precipitation in modern microbial mats. *Earth-Science Reviews* **96**, 141–162.

Edgcomb VP, Bernhard JM, Beaudoin D, Pruss S, Welander PV, Schubotz F, Mehay S, Gillespi AL, Summons RE (2013) Microbial diversity in oolitic sands of Highborne Cay, Bahamas. *Geobiology* **11**, 234–251.

Folk RL, Lynch FL (2001) Organic matter, putative nannobacteria, and the formation of ooids and hardgrounds. *Sedimentology* **48**, 215–229.

Fournier M, Dermoun Z, Durand M, Dolla A (2004) A new function of the *Desulfovibrio vulgaris* Hildenborough [Fe] hydrogenase in the protection against oxygen stress. *Journal of Biological Chemistry* **273**, 1787–1793.

Gao H, Schreiber F, Collins G, Jensen MM, Kostka JE, Lavik G, de Beer D, Zhou H, Kuypers MMM (2010) Aerobic denitrification in permeable Wadden Sea sediments. *ISME Journal* **4**, 417–426.

Gaudain G, Medley P (2000) The Turks and Caicos Islands. In *Seas at the Millennium: An Environmental Evaluation* (ed. Sheppard C). Pergamon, Amsterdam, pp. 587–594.

Gerdes G, Krumbein WE (1987) Biolaminated deposits of benthic microbial communities. In *Lecture Notes in Earth Science* (eds Bhattacharya GM, Friedmann GM, Neugebauer H, Seilacher A). **9**, pp. 1–183.

Gerdes G, Dunajtschik-Piewak K, Riege H, Taher AG, Krumbein WE, Reinick HH (1994) Structural diversity of biogenic carbonate particles in microbial mats. *Sedimentology* **41**, 1273–1294.
Golubic S, Radke G, Le Campion-Alsumard T (2005) Endolithic fungi in marine ecosystems. *Trends in Microbiology* **13**, 229–235.
González R, Eberli GP (1997) Sediment transport and sedimentary structures in a carbonate tidal inlet; Lee Stocking Island, Exumas Islands, Bahamas. *Sedimentology* **44**, 1015–1030.
Grubbs F (1969) Procedures for detecting outlying observations in samples. *Technometrics* **11**, 469–479.
Harris PM (1979) Facies anatomy and diagenesis of a Bahamian ooid shoal. *Sedimenta* **7**, 1–169.
Harris PM (1983) The Joulters ooid shoal, Great Bahama Bank. In *Coated Grains* (ed. Peryt TM). Springer-Verlag, New York, pp. 132–141.
Harris PM (2010) Delineating and quantifying depositional facies patterns in carbonate reservoirs: Insight from modern analogs. *AAPG Bulletin* **94**, 61–68.
Harris PM, Halley RB, Lukas KJ (1979) Endolith microborings and their preservation in Holocene-Pleistocene (Bahama-Florida) ooids. *Geology* **7**, 216–220.
He Z, Gentry TJ, Schadt CW, Wu L, Liebich J, Chong SC, Huang Z, Wu W, Gu B, Jardine P, Criddle C (2007) GeoChip: a comprehensive microarray for investigating biogeochemical, ecological and environmental processes. *ISME Journal* **1**, 67–77.
Hügler M, Sievert SM (2011) Beyond the Calvin Cycle: Autotrophic carbon fixation in the ocean. *Annual Reviews in Marine Science* **3**, 261–289.
Hunter EM, Mills HJ, Kostka JE (2006) Microbial community diversity associated with carbon and nitrogen cycling in permeable shelf sediments. *Applied and Environmental Microbiology* **72**, 5689–5701.
Jørgensen BB (1982) Mineralization of organic matter in the seabed — the role of sulphate reduction. *Nature* **296**, 643–645.
Kahle CF (1977) Origin of marine ooids: evidence from the Pleistocene Miami Limestone, Florida Keys [abs.]: *Geological Society of America North-Central Meeting abstracts.*
Kahle CF (2007) Proposed origin of aragonite Bahamian and some Pleistocene marine ooids involving bacteria, nannobacteria and biofilms. *Carbonates and Evaporites* **22**, 10–22.
Karl D, Michaels A, Bergman B, Capone D, Carpenter E, Letelier R, Lipschultz F, Paerl H, Sigman D, Stal L (2002) Dinitrogen fixation in the world's oceans. *Biogeochemistry* **57/58**, 47–98.
Kawaguchi T, Decho AW (2002) Isolation and biochemical characterization of extracellular polymers (EPS) from modern soft marine stromatolites: inhibitory effects on $CaCO_3$ precipitation. *Preparative Biochemistry and Biotechnology* **32**, 51–63.
Keith BD, Zuppann CW (1993) Mississippian oolites and modern analogs. *AAPG Studies in Geology* **35**, 265.
King GM, Weber CF (2007) Distribution, diversity and ecology of aerobic CO-oxidizing bacteria. *Nature Reviews Microbiology* **5**, 107–118.
Krekeler D, Teske A, Cypionka H (1998) Strategies of sulfate-reducing bacteria to escape oxygen stress in a cyanobacterial mat. *FEMS Microbiology Ecology* **25**, 89–96.
Kuhl MM, Jorgensen BB (1992) Microsensor measurements of sulfate reduction and sulfide oxidation in compact microbial communities of aerobic biofilms. *Applied and Environmental Microbiology* **58**, 1164–1174.
Ley RE, Harris JK, Wilkox J, Spear JR, Bebout BM, Maresca JA, Bryant DA, Sogin ML, Pace NR (2006) Unexpected diversity and complexity of the Guerrero Negro hypersaline microbial mat. *Applied and Environmental Microbiology* **72**, 3685–3695.
Liang Y, Li G, Van Nostrand JD, He Z, Wu L, Deng Y, Zhang X, Zhou J (2009) Microarray-based analysis of microbial functional diversity along an oil contamination gradient in oil field. *FEMS Microbiology Ecology* **70**, 324–333.
Liang Y, He Z, Wu L, Deng Y, Li G, Zhou J (2010) Development of a common oligo reference standard (CORS) for microarray data normalization and comparison across different microbial communities. *Applied and Environmental Microbiology* **76**, 1088–1094.
Lindqvist A, Membrillo-Hernańdez J, Poole RK, Cook GM (2000) Roles of respiratory oxidases in protecting *Escherichia coli* K12 from oxidative stress. *Antonie van Leeuwenhoek* **78**, 23–31.
Lindsay RF, Cantrell DL, Hughes GW, Keith TH, Mueller HW, Russell SD (2006) Ghawar Arab-D reservoir: Widespread porosity in shoaling upward-cycles, Saudi Arabia. In *Giant Hydrocarbon Reservoirs of the World: From Rocks to Reservoir Characterization* (eds Harris PM, Weber LJ). AAPG Memoir, Tulsa, OK, **88**, pp. 97–138.
Lombard J, Moreira D (2011) Early evolution of the biotin-dependent carboxylase family. *BMC Evolutionary Biology* **11**, 232.
Loreau JP, Purser BH (1973) Distribution and ultrastructure of Holocene ooids in the Persian Gulf. In *The Persian Gulf—Holocene Carbonate Sedimentation and Diagenesis in a Shallow Epicontinental Sea* (ed. Purser BH). Springer-Verlagg, Berlin, pp. 279–328.
Lorite M, Tachil J, San Juan J, Meyer O, Bedmar EJ (2000) CODH activity in *Bradyrhizobium japonicum. Applied and Environmental Microbiology* **66**, 1871–1876.
Lu Z, Deng Y, Van Nostrand JD, He Z, Voordeckers J, Zhou A, Lee Y, Mason O, Dubinsky E, Chavarria K, Tom L, Fortney J, Lamendella R, Jansson JK, D'haeseleer P, Hazen TC, Zhou J (2012) Microbial gene functions enriched in the Deepwater Horizon deep-sea oil plume. *ISME Journal* **6**, 451–460.
Ludwig R, Al-Horani FA, de Beer D, Jonkers HM (2005) Photosynthesis – controlled calcification in a hypersaline microbial mat. *Limnology and Oceanography* **50**, 1836–1843.
Milliman JD (1993) Production and accumulation of calcium carbonate in the ocean: budget of a non-steady state. *Global Biogeochemical Cycles* **7**, 927–957.
Milliman JD, Droxler AW (1995) Calcium carbonate sedimentation in the global ocean: linkages between the neritic and pelagic environments. *Oceanography* **8**, 92–94.
Mills J, Hunter E, Humphrys M, Kerkhof L, McGuinness L, Huettel M, Kostka JE (2008) Characterization of nitrifying, denitrifying, and overall bacterial community structure in permeable marine sediments of the Northeastern Gulf of Mexico. *Applied & Environmental Microbiology* **74**, 4440–4453.
Mitterer RM (1968) Aminoacid composition of organic matrix in calcareous oolites. *Science* **162**, 498–1499.
Mobberley JM, Khodadad CLM, Foster JS (2013) Metabolic potential of lithifying cyanobacteria-dominated thrombolitic mats. *Photosynthesis Research* **118**, 125–140.
Morse JW, Mackenzie FT (1990) Geochemistry of sedimentary carbonates. *Developments in Sedimentology* **48**, 696.
Pacton M, Ariztegui D, Wacey D, Kilburn MR, Rollion-Bard C, Farah R, Vasconcelos C (2012) Going nano: a new step toward understanding the processes governing freshwater ooid formation. *Geology* **40**, 547–550.
Paerl HW, Prufert LE (1987) Oxygen-poor microzones as potential sites of microbial nitrogen fixation in nitrogen-depleted aerobic marine waters. *Applied and Environmental Microbiology* **53**, 1078–1087.

Park SW, Park ST, Lee JE, Kim YM (2008) *Pseudonocardia carboxydivorans* sp. Nov., a CO oxidizing actinomycete and an embedded description of the genus *Pseudonocardia*. *International Journal of Systematic and Evolutionary Microbiology* **58**, 2475–2478.

Perkins RG, Patterson DM, Sun H, Watson J, Player MA (2004) Extracellular polymeric substances: quantification and use in erosion experiments. *Continental Shelf Research* **24**, 1623–1635.

Petrie M (2010) Sedimentology of a grain-dominated tidal flat, tidal delta, and eolianite system: Shroud Cay, Exumas, Bahamas. MS thesis, University of Miami, 277 pp. unpublished.

Piggot AM, Klaus JS, Johnson S, Phillips M, Solo-Gabriele HM (2012) Relationship between enterococcal levels and sediment biofilms at recreational beaches in South Florida. *Applied and Environmental Microbiology* **17**, 5973–5982.

Plée K, Ariztegui R, Martin R, Davaud E (2008) Unravelling the microbial role in ooid formation- results of an in situ experiment in modern freshwater Lake Geneva in Switzerland. *Geobiology* **6**, 341–350.

Plée K, Pacton M, Ariztegui D (2010) Discriminating the role of photosynthetic and heterotrophic microbes triggering low-Mg calcite precipitation in freshwater biofilms (Lake Geneva, Switzerland). *Geomicrobiology Journal* **27**, 391–399.

Rankey EC, Reeder SL (2009) Holocene ooids of Aitutaki Atoll, Cook Islands, South Pacific. *Geology* **37**, 971–974.

Rankey EC, Riegl B, Steffen K (2006) Form, function, and feedbacks in a tidally dominated ooid shoal, Bahamas. *Sedimentology* **53**, 1191–1210.

Reeder SL, Rankey EC (2008) Relations between sediments and tidal flows in ooid shoals, Bahamas. *Journal of Sedimentary Research* **78**, 175–186.

Ries JB, Anderson MA, Hill RT (2008) Seawater Mg/Ca controls polymorph mineralogy of microbial $CaCO_3$: a potential proxy for calcite-aragonite seas in Precambrian time. *Geobiology* **6**, 106–119.

Robbins LL, Yates KK, Shinn E, Blackwelder P (1996) Whitings on the Great Bahama Bank: A microscopic solution to a macroscopic mystery. *Bahamas Journal of Science* **4**, 1–7.

Sieburth JM (1976) Bacterial substrates and productivity in marine ecosystems. *Annual Reviews in Ecology and Systematics* **7**, 259–285.

Sigalevich P, Baev MV, Teske A, Cohen Y (2000) Sulfate reduction and possible aerobic metabolism of the sulfate-reducing bacterium *Desulfovibrio oxyclinae* in a chemostat coculture with *Marinobacter* sp. strain MB under exposure to increasing oxygen conditions. *Applied and Environmental Microbiology* **66**, 5013–5018.

Smith NP (1995) On long-term net flow over Great Bahama Bank. *Journal of Physical Oceanography* **25**, 679–684.

Strauss G, Fuchs G (1993) Enzyme of a novel autotrophic CO2 fixation pathway in the phototrophic bacterium *Chloroflexus aurantiacus*, the 3-hydroxypropionate cycle. *European Journal of Biochemistry* **215**, 633–643.

Summons RE, Bird LR, Gillespie AL, Pruss SB, Roberts M, Sessions AL (2013) Lipid biomarkers in ooids from different locations and ages: evidence for a common bacterial flora. *Geobiology* **5**, 420–436.

Underwood GJC, Patterson DM, Parkes RJ (1995) The measurement of microbial carbohydrate exopolymers form intertidal sediments. *Limnology and Oceanography* **40**, 1243–1253.

Visscher PT, Stolz JF (2005) Microbial mats as bioreactors: populations, processes and products. *Palaeogeography and Palaeoclimatology* **219**, 87–100.

Visscher PT, Gritzer RF, Leadbetter ER (1999) Low molecular weight sulfonates, a major substrate for sulfate reducers in marine microbial mats. *Applied and Environmental Microbiology* **65**, 3272–3278.

Visscher PT, Reid RP, Bebout BM (2000) Microscale observations of sulfate reduction: correlation of microbial activity with lithified micritic laminae in modern marine stromatolites. *Geology* **28**, 919–922.

Wang F, Zhou H, Meng J, Peng X, Jiang L, Sun P, Zhang C, Van Nostrand JD, Deng Y, He Z, Wu L, Zhou J, Xiao X (2009) GeoChip-based analysis of metabolic diversity of microbial communities at the Juan de Fuca Ridge hydrothermal vent. *Proceeding of the National Academy of Science of the USA* **106**, 4840–4845.

Wang J, Van Nostrand JD, Wu L, He Z, Li G, Zhou J (2011a) Microarray-based evaluation of whole community genome amplification methods. *Applied and Environmental Microbiology* **77**, 4241–4245.

Wang H, He J, Ma F, Yang K, Wei L (2011b) Aerobic denitrification of a *Pseudomonas* sp. isolated from a high strength ammonium wastewater treatment facility. *Science Research and Essays* **6**, 748–755.

Ward WC, Brady MJ (1973) High-enegy carbonates on their inner shelf, northeastern Yucatan Peninsula, Mexico. *Transactions of the Gulf Coast Association of Geological Societies* **23**, 226–238.

Wu L, Liu X, Schadt CW, Zhou J (2006) Microarray-based analysis of submicrogram quantities of microbial community DNAs by using whole-community genome amplification. *Applied and Environmental Microbiology* **72**, 4931–4941.

Wu L, Kellogg L, Devol AH, Tiedje JM, Zhou J (2008) Microarray-based characterization of microbial community functional structure and heterogeneity in marine sediments from the Gulf of Mexico. *Applied and Environmental Microbiology* **74**, 4516–4529.

Zarzycki J, Brecht V, Muller M, Fuchs G (2009) Identifying the missing steps of the autotrophic 3-hydroxypropionate CO2 fixation cycle in *Chloroflexus aurantiacus*. *Proceeding of the National Academy of Science of the USA* **106**, 21317–21322.

Zehr JP, Kudela RM (2011) Nitrogen cycle of the open Ocean. *Annual Review of Marine Science* **3**, 197–225.

Zhang W, Sileica TS, Chen C, Liu Y, Lee J, Packman AI (2011) A novel planar flow cell for studies of biofilm heterogeneity and flow biofilm interactions. *Biotechnology and Bioengineering* **11**, 2571–2582.

Zhang Y, Lu Z, Liu S, Yang Y, He Z, Ren Z, Zhou J, Li D (2013) Geochip-based analysis of microbial communities in alpine meadow soils in the Qinghai-Tibetan plateau. *BMC Microbiology* **13**, 72.

SUPPORTING INFORMATION

Additional Supporting Information may be found in the online version of this article:

Fig. S1 Relative abundance of phylogenetic groups associated with autotrophic carbon fixation. (A) pcc/acc (propionyl-CoA/acetyl-CoA carboxylase); (B) RuBisCO ribulose (1,5-biphosphate carboxylase/oxygenase); (C) carbon monoxide dehydrogenase (CODH); (D) *aclB-ATP* (ATP citrate lyase). Relative abundance is based on the total signal intensities of all genes associated with each particular carbon fixation pathway. *Proteobacteria* phylum is divided into the classes, *Alpha-*, *Beta-*, *Gamma-*, *Epsilon-*.

Fig. S2 Phylogenetic distribution and normalized signal intensity of genes associated with representative microbial genera associated with acetogenesis and methanotrophy. (A) Representative distribution of acetogens at phylum level. *Proteobacteria* phylum is divided into the classes, *Alpha-* and *Gamma-*; (B) Distribution of acetogens at genus level. *Proteobacteria* phylum is divided into the classes, *Alpha-*, *Beta-*, *Gamma-*; (C) Distribution of methanotrophs at phylum level; and (D) Distribution of methanotrophs at genus level. Relative abundance is based on the total signal intensities of genes associated with each particular geochemical cycle.

Fig. S3 Phylogenetic distribution of genes associated with denitrification. (A) Representative distribution of denitrifiers at phylum level. *Proteobacteria* phylum is divided into the classes, *Alpha-*, *Beta-*, *Gamma-*; (B) Distribution of denitrifiers at genus level. Relative abundance is based on the total signal intensities of all denitrification genes within a given phylogenetic group.

Fig. S4 Phylogenetic distribution of genes involved in ammonification. Relative abundance is based on the total signal intensities of all genes associated with ammonification. *Proteobacteria* phylum is divided into the classes, *Alpha-*, *Beta-*, *Delta-*, *Gamma-*.

Fig. S5 Phylogenetic distribution of genes associated with N_2 fixation. (A) Representative distribution of N_2- fixers at phylum level. *Proteobacteria* phylum is divided into the classes, *Alpha-*, *Beta-*, *Delta-*, *Epsilon-*. (B) Distribution of N_2 fixers at genus level. Relative abundance is based on the total signal intensities of N_2 fixation genes within a given phylogenetic group.

Fig. S6 Phylogenetic distribution of genes associated with sulfate reduction. (A) Representative distribution of sulfate reducers at phylum level. *Proteobacteria* phylum is divided into the classes, *Alpha-*, *Beta-*, *Delta-*, *Gamma-*. (B) Distribution of sulfate reducers at genus level. Relative abundance is based on the total signal intensities of sulfate-reducing genes within a given phylogenetic group.

Table S1 Summary of GEOCHIP 4.2 probes and covered gene sequences among different categories.